

A Systematic Performance Analysis of Deep Perceptual Loss Networks: Breaking Transfer Learning Conventions

Gustav Grund Pihlgren*, Konstantina Nikolaidou†, Prakash Chandra Chhipa†, Nosheen Abid†, Rajkumar Saini†, Fredrik Sandin†, Marcus Liwicki†

**Explainable AI Group*

Umeå University, Sweden
gustav.pihlgren@umu.se

† *Machine Learning Group*

Luleå University of Technology, Sweden
{firstname}.{lastname}@ltu.se

Abstract—Deep perceptual loss is a type of loss function in computer vision that aims to mimic human perception by using the deep features extracted from neural networks. In recent years, the method has been applied to great effect on a host of interesting computer vision tasks, especially for tasks with image or image-like outputs, such as image synthesis, segmentation, depth prediction, and more. Many applications of the method use pretrained networks, often convolutional networks, for loss calculation. Despite the increased interest and broader use, more effort is needed toward exploring which networks to use for calculating deep perceptual loss and from which layers to extract the features.

This work aims to rectify this by systematically evaluating a host of commonly used and readily available, pretrained networks for a number of different feature extraction points on four existing use cases of deep perceptual loss. The use cases of perceptual similarity, super-resolution, image segmentation, and dimensionality reduction, are evaluated through benchmarks. The benchmarks are implementations of previous works where the selected networks and extraction points are evaluated. The performance on the benchmarks, and attributes of the networks and extraction points are then used as a basis for an in-depth analysis. This analysis uncovers insight regarding which architectures provide superior performance for deep perceptual loss and how to choose an appropriate extraction point for a particular task and dataset. Furthermore, the work discusses the implications of the results for deep perceptual loss and the broader field of transfer learning. The results show that deep perceptual loss deviates from two commonly held conventions in transfer learning, which suggests that those conventions are in need of deeper analysis.

I. INTRODUCTION

In the last decade, machine learning for computer vision has evolved significantly. This evolution is mainly due to the developments in artificial neural networks. An essential focus of these developments has been the calculation of the loss used to train models. One group of loss functions build on using a neural network to calculate the loss for another machine learning model. Among these methods are milestone achievements such as adversarial examples [1], generative adversarial networks [2], and deep visualization [3]. The neural

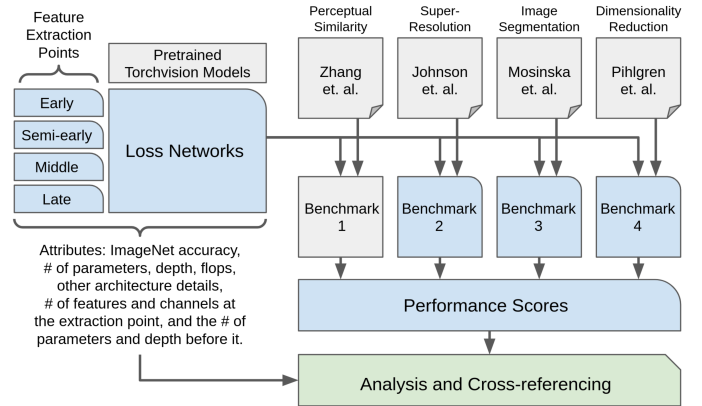


Fig. 1. The procedure followed in this work. This work investigates the effect of loss networks with different ImageNet [4] pretrained architectures and feature extraction points on the downstream performance of deep perceptual loss and similarity tasks. Loss networks with 14 pretrained architectures are examined for four different feature extraction points by evaluating them on four benchmarks based on experiments from prior works [5, 6, 7, 8]. The performance and attributes of each loss network are analysed and cross-referenced with the other loss networks to uncover which attributes are correlated with performance and other trends. This work makes novel contributions (blue, round-corner) regarding feature extraction points, systematic analysis of loss networks, and systematic evaluation on Benchmark 2 through 4. The major contribution of this work (green, cut-corner) is the large analysis and cross-reference if the attributes and performance scores.

networks that are being used during loss calculation in this way are often called loss networks.

One of the methods that makes use of loss networks that have proven effective for a range of computer vision applications is deep perceptual loss. Deep perceptual loss aims to create loss functions for machine learning models that mimic human perception of similarity. This is typically done by calculating the similarity of the output image and ground truth by how similar the deep features (activations) of the loss network are when either image is used as input. This method of similarity measurement is known as deep perceptual similarity, and when

used as part of a loss function it is known as deep perceptual loss.

Deep perceptual loss is well suited for image synthesis, where it is utilized to improve performance on various tasks. These tasks include style-transfer [9], image generation [10], super-resolution [6], image denoising [11], and more. In addition to image synthesis, the method has been successful for tasks with image-like outputs such as image segmentation [12], dimensionality reduction [13], and image depth prediction [14]. Additionally, deep perceptual similarity has become one of the dominant techniques for measuring the perceptual similarity of images [5, 15].

Despite the diverse and widespread use of deep perceptual loss and similarity, how to implement a suitable loss network for a given task remains unexplored. The choice of loss network architectures used in prior works has either been justified by prior use [13, 14] or not at all [9, 16, 6, 7, 12, 8]. However, some rare exceptions give justifications based on hypotheses regarding the suitability of the architecture to the given data [17], though these hypotheses are not actually tested. Furthermore, the choice of extraction points also typically lacks justification [6, 12, 8, 14]. In the cases when a justification does exist it is usually not tested [9, 16, 13] or limited to similar layers [7]. With the increasing use of deep perceptual loss, a study into improved loss network selection is well justified, which is the purpose of this work.

A. Scope

There are many aspects to consider when implementing a loss network for deep perceptual loss. There is an abundance of neural network architectures available, plenty of datasets that could be used to train them, and a plethora of ways to perform feature extractions from those networks. It is clearly outside the scope of any one study to look into them all.

This work investigates how the selection of pretrained architecture and feature extraction points affects the performance of loss networks when used on different deep perceptual loss tasks. It does this by systematically testing a wide variety of easily accessible and well-known pretrained Convolutional Neural Networks (CNNs) architectures and comparing their performance as loss networks with four different extraction points. The performance is evaluated on four prior works that have used pretrained loss networks [5, 6, 7, 8]. The experiments of those previous works are used as benchmarks where the original loss networks have been replaced with the ones examined in this work. The results obtained from these benchmark experiments have been analyzed to gain insight into how the choice of architecture and feature extraction point affects performance. These insights have been the basis for further suggestions on how to select pretrained architectures and extraction points for loss networks. An illustration of the procedure followed in this work, from the four prior works and loss networks to the analysis, is shown in Fig 1.

The four benchmarks represent four different applications of loss networks. Benchmark 1 [5] evaluates the loss networks as a perceptual similarity metrics on the BAPPS dataset. Benchmark 2 [6] evaluates image transformation networks trained

for super-resolution with the loss networks on the Set5 [18], Set14 [19] and BSD100 [20] datasets. Benchmark 3 [7] evaluates U-nets [21] trained with the loss networks on the MRD dataset [22]. Benchmark 4 [8] evaluates autoencoders trained with the loss networks by the performance of MLPs trained to perform classification using the learned embeddings on the SVHN [23] and STL-10 [24] datasets. For each benchmark a set of performance scores are gathered for each loss network. Details regarding the four benchmarks and justification for their use can be found in Section IV.

This work focuses on the use of pretrained networks as they are by far the most common use of deep perceptual loss and easier to implement. The pretrained models selected for evaluation are some of the classification architectures provided by Torchvision [25], a package of the PyTorch [26] framework. All of the selected models have been pretrained with the ImageNet [4] dataset. These networks, with or without pretrained parameters, are readily available for public use, which is itself a motivation for their usage; however, there are more reasons for using the networks provided in Torchvision. The pretrained neural networks available in Torchvision contain a wide variety of architectures based on several renowned papers [27, 28, 29, 30, 31]. There are also multiple different implementations of the different networks within Torchvision. This provides the ability to test how different architectures behave as loss networks and how this behavior changes with more minor changes in implementation. Additionally, applications of deep perceptual loss commonly use the pretrained networks in Torchvision to create loss networks.

Another limitation in scope is that only models pretrained on ImageNet are used in the loss networks. While exploring how different pretraining procedures and datasets affect the loss networks is an interesting proposition, this is left for future works to investigate. Aside from ease of access, the ImageNet dataset is a good choice for loss network pretraining as it is the most popular pretraining dataset for deep perceptual loss. Additionally, it is one of the largest and most well-used computer vision datasets.

This work also investigates how the choice of the layers in the loss networks that feature extractions are made from affects the trained models. The impact of different layers for feature extraction has often been left out of prior works and no systematic evaluation has been conducted. Since the feature extraction points used for a loss network can be changed without needing to retrain the network this aspect can be explored without adding much more computational demand to the experiments.

In this work, the loss networks extract features in a straightforward manner. For a given architecture and extraction point, the activations are propagated forward to the extraction point and then used directly to calculate the loss, as further detailed in Section III. While more elaborate feature extraction methods exist, they are not considered in this work.

B. Contributions

This work has produced a large amount of data covering the attributes and performance scores of the loss networks.

The complete collection of data is made available in the supplementary material found in the Appendix, and the complete implementation of the experiments is available online¹. Analysis of the attributes and performance scores gives insight into which architectures and extraction points that provide good performance for a given task and dataset. The findings include that VGG networks without batch normalization (batch norm) give the best performance among the tested architectures and that the choice of feature extraction point is at least as important as choice of architecture. The analysis also reveals that deep perceptual loss do not adhere to two conventions of transfer learning. The conventions that better ImageNet accuracy implies better downstream performance and that feature extraction from the later layers provide better performance. Based on the findings and analysis, suggestions for future work are made including further analysis of loss networks, lacking overarching studies for deep perceptual loss, and reevaluation of transfer learning conventions.

II. BACKGROUND

The terminology of the subfield of perceptual loss is only sometimes used consistently between pieces of literature. For clarity, this section is prefaced with a description of how some standard terms are used in this work. Additionally, these terms are introduced with greater detail throughout the literature review.

- A perceptual loss is a loss function that is meant to estimate a factor of human perception, often to have model predictions be closer to those of humans.
- A loss network is a neural network used as part of the loss calculation for training another machine learning model. For cohesion, this work also uses the term loss network to refer to networks used to compute image similarity.
- Deep perceptual loss is when the deep features of a loss network are used to calculate the perceptual loss of another machine learning model by comparing the deep features generated by the model output to those generated by the ground truth.

A. Feature Extraction

Feature extraction in machine learning is the process of converting input data into descriptive and non-redundant features. Before feature learning became widely adopted, most feature extraction methods relied on task-related features handcrafted by experts [32]. However, with the advancement of the deep models and autoencoders [33, 34], feature extraction has been automated to cater to complex invariances in the data [35]. Feature extraction using deep models has been successfully used in many applications like image classification [32, 36, 37], cross-media retrieval [38], and brain tumors classification [39].

However, determining an architecture for feature extraction and how to pretrain the network is difficult, and the best practice often varies among fields and individual tasks. Generally, for many computer vision tasks, the trend has been to use

pretrained models based on ImageNet [4] which, in general, has improved downstream performance [40, 41]. Nevertheless, it has also been shown that for unsupervised pretraining, better pretraining performance does not always lead to better downstream performance [42]. As such it can be difficult to tell what feature extraction methods will perform well on a given task without prior evaluation.

B. Perceptual Similarity Metrics

A field that has made use of the deep features of image-processing neural networks is image similarity metrics. Image similarity metrics are designed to measure the similarity or difference between two images. A class of image similarity metrics that has often been used in machine learning is pixel-wise metrics.

Pixel-wise similarity metrics work by aggregating the differences between each pair of corresponding pixels between two images. This aggregation is often performed through standard distance functions like mean square error or log-likelihood. However, pixel-wise metrics are widely known to be flawed measurements of similarity, especially when estimating human perception [10]. For example, they do not take into account the relations between different pixels or the differing importance of various pixel regions [13].

To mitigate the flaws of pixel-wise metrics, several metrics have been proposed that estimate human perception of visual similarity, so-called perceptual similarity. Among these perceptual similarity metrics are some that have become widely used for computer vision applications such as the Structural Similarity Index Measure (SSIM) [43]. With the advent of deep learning, the deep features extracted by neural networks from the input images was used to do similarity comparison for content-based image retrieval [44] and later applied as a perceptual similarity metric [5]. The method has been further improved by Ding *et al.*, [15] which took inspiration from neural style transfer [9] and use the network to calculate both texture and content similarity. This use of deep neural networks as perceptual similarity metrics is called deep perceptual similarity.

Deep perceptual similarity metrics commonly make use of pretrained networks. Training the networks specifically for perceptual similarity can give a small increase in performance [5], especially when used together with ensemble methods [45]. However, this improvement is marginal at best, which attests to how effective the deep features of pretrained CNNs are for perceptual similarity.

A recent study analyzed how different network architectures and pretraining methods affect performance in the context of deep perceptual similarity [41]. This recent study shares similarities in methodology to the present work; however, it did not examine deep perceptual loss. The results of this recent study indicated that better pretraining performance does not necessarily lead to an improved perceptual similarity metric. In fact, after a certain point, enhanced pretraining performance was shown to be detrimental to the perceptual similarity results. The upper bound of the perceptual similarity performance as a function of ImageNet accuracy was shown to gradually increase

¹<https://github.com/LTU-Machine-Learning/Analysis-of-Deep-Perceptual-Loss-Networks>

until a certain threshold, after which the performance decreased. While prior studies have also shown limited correlations between the pretraining and downstream performance [42], the clear performance increase until a certain point followed by a clear decrease is a surprising result. Moreover, previous works have shown that the selected model and pretraining strategy substantially impact the perceptual similarity results [41]. Thus, selecting the appropriate architecture and pretraining procedure is more important than any training step involving actual perceptual similarity data.

C. Deep Perceptual Loss

In machine learning models trained with image data as the ground-truth, it is common to use pixel-wise metrics to calculate so-called pixel-wise loss [10]. However, in recent years the flaws of pixel-wise metrics have been considered with respect to loss calculation [10, 13]. Perceptual losses, based on perceptual similarity metrics, have been proposed as an alternative or complement to pixel-wise losses by using perceptual similarity metrics as part of the loss calculation. For example, SSIM was adapted as a perceptual loss function [46, 47].

One of the most popular and widespread groups of perceptual losses are those based on deep perceptual similarity, so-called deep perceptual loss. Deep perceptual loss was first used with neural style transfer [9] where features from a pretrained version of VGG-19 [48] were used to estimate perceptions of style and content. These perceptions were then used as a loss to generate images with the perceived content of one image and the perceived style of another. Since its introduction, deep perceptual loss has been a popular tool for image-generation tasks. It was used in the VAE-GAN (variational autoencoder, generative adversarial network) in which the discriminator acts as a loss network to facilitate higher quality image generation [10]. In the VAE-GAN, the discriminator is trained alongside the generator; however, other works have used pretrained loss networks instead, removing the need for extra training [16].

Other popular uses tend to be adjacent to the image generation domain, where the output of the model is a 2-dimensional lattice such as image segmentation [7], feature heat maps for object detection [49], and depth prediction [14]. This is not so surprising as deep perceptual loss was first developed in the computer vision domain and tends to use models pretrained on images as loss networks. As such, the deep features of these networks are more useful when extracted from images and image-like inputs.

However, not all models that output 2-dimensional lattices during training are used for that purpose. Convolutional autoencoders, for example, are often used for dimensionality reduction instead of image generation. Deep perceptual loss has been proven effective in this case as well [13].

Despite the many applications and growing use of deep perceptual loss, there has been relatively little effort in investigating how to best utilize the method. Most works pick a pretrained architecture without further investigation. Rare works investigate a few different models [16] or a few different feature extraction points [7]. While studies exist that cover

how useful different models are for general feature learning applications [50, 40, 51] and deep perceptual similarity [41], no such studies exist for deep perceptual loss.

D. Applications

Deep perceptual loss is frequently used in image synthesis tasks like image fusion [17], style-transfer [6], and super-resolution [52]. Deep perceptual loss has also been adapted for better results in many domains like medical images [11] and earth observation [53]. In addition to analyzing deep perceptual similarity, this work focuses on three applications of deep perceptual loss.

The first application considered in this work is super-resolution transformation. In super-resolution, a deep perceptual loss function can be used to compare an upscaled output image with a known full-scale image. The second application involves image delineation, a type of image segmentation. This application uses a deep perceptual loss function to calculate the difference between the output and desired segmentation results. The third application is dimensionality reduction for downstream tasks with autoencoders. Here, a deep perceptual loss function calculates the similarity between the output image of an autoencoder and the original image as part of the so-called reconstruction loss. The three applications of deep perceptual loss are described in more detail below.

1) *Super-resolution*: Super-resolution is the task of transforming a low-resolution image into a high-resolution image. The practicality of super-resolution models has been demonstrated in real-world applications such as security [54] and medical image processing [55, 56]. Moreover, a super-resolution model can be combined with other algorithms or models to enhance the performance of different computer vision tasks [57, 58], such as object detection [59] and pose estimation [60]. Similar to image segmentation tasks, the deep perceptual loss has been widely adopted to train super-resolution models [6, 61], including in important medical applications [11].

2) *Image segmentation*: Image segmentation involves dividing an image into different segments representing classes or instances at the pixel level. Each pixel in the image is assigned a class or instance, and the resulting segmentation model output is a 2D lattice that can be interpreted as an image. Deep perceptual loss has been used to train segmentation models in applications such as delineating roads in aerial images, locating cracks in roads identifying the edges of cells in microscope images [7], and segmenting medical images [12].

3) *Autoencoding*: Autoencoders have been used for decades as a tool for dimensionality reduction and feature learning [62, 63]. They have also been used for purposes beyond dimensionality reduction, such as image generation [64]. In the last couple of years, deep perceptual loss has been used to train autoencoders for image generation [10] and more recently also for their original dimensionality reduction purposes [13].

E. Pretrained Torchvision networks

The Torchvision package [25] provides many different renowned CNN architectures that have been pretrained on the

ImageNet dataset [4]. Many of these CNN architectures have won challenges and awards like ILSVRC-2012 [4], ILSVRC-2014 competition, and CVPR award 2017. This section briefly covers the accomplishments, innovations, and general design of the architectures found in Torchvision that are used in this work. However, this section does not go into implementation details for each of the networks. For such information, the reader is referred to the works that introduced those architectures. The ImageNet accuracy as well as some attributes of the pretrained models used can be found in Table I. The investigated Torchvision architectures are described below.

1) *AlexNet*: AlexNet is the name given to the network introduced by Krizhevsky et al. [27] and further built upon in [28]. While AlexNet has lower performance and robustness than more recent CNN architectures [70], its features have proven competitive to those same networks when used as a perceptual similarity metric [5].

2) *VGG*: VGG is an innovative object-detection deep model proposed by Simonyan and Zisserman in 2012 [29]. It is a CNN that is one of the best object-detection models even today. VGG uses small-size convolution filters that allow the integration of more weighted layers. This work explores some of its versions, namely, VGG-11, VGG-16, VGG-19, and a version of VGG-16 that uses batch normalization (batch norm) called VGG-16_bn.

3) *Residual Networks*: To solve the problem of vanishing or exploding gradients in very deep networks, residual networks (ResNet) using skip connections were introduced [30]. Skip connections connect later layers to earlier ones skipping some layers in between. There are many updated versions of ResNet introduced later to improve the performance. One of the subsequent versions, called ResNeXt-50, redesigned the fundamental building block of ResNet to use a multi-branch setup similar to inception networks [65].

This work has worked with three types of residual networks, namely, ResNet-18, ResNet-50, and ResNeXt-50 32x4d.

4) *SqueezeNet*: While much of the contemporary research on deep CNNs focused on improving the performance, Iandola et al., [69] focused on reducing the size of deep models by proposing SqueezeNet. It has a similar performance to AlexNet with 50 times fewer parameters. To achieve these benefits, SqueezeNet has reduced the kernels with size 3 to 1×1 convolutions, used squeeze layers to decrease the number of input channels to the kernels, and downsample later in the architecture to have large activation maps with the assumption that it leads to higher classification accuracy.

5) *Inception Networks*: Choosing the appropriate filter size for different layers in a CNN architecture can be challenging. If the filter size is large, it may lose the distribution locally; if the filter is small, it may lose the information distributed globally. Inception networks [31] were introduced to handle this issue by using multiple filter sizes at each layer, leading the networks to be "wider" rather than "deeper". Inception networks have achieved state-of-the-art performance on image classification. This work explores the first version of Inception Network developed by the Google team, i.e., GoogLeNet [31] and Inception Network version 3 [66].

6) *DenseNet*: DenseNet [68] focused on using fewer parameters with densely connected layers to achieve higher accuracy. It is composed of dense blocks. Each layer in the dense block takes the feature maps of preceding layers as input. This concept of DenseNet reduces the vanishing gradient problem, improves feature propagation, stimulates feature reuse, and considerably reduces the number of parameters. In this work, the DenseNet-121 implementation is examined.

7) *EfficientNet*: EfficientNet [67] is a CNN-based architecture that uses compound coefficients to scale the architecture's dimensions uniformly. Unlike traditional methods that arbitrarily scale these factors, a set of fixed scaling coefficients is used to scale the networks in a principled way uniformly. This method combined with neural architecture search [71] produced the state-of-the-art EfficientNet architectures. In this work, the two versions of EfficientNet with the fewest and most layers are explored, i.e., EfficientNet_B0 and EfficientNet_B7.

III. LOSS NETWORKS AND FEATURE EXTRACTION

The primary goal of this work is to explore how using different pretrained architectures and feature extraction points affects the implemented experiments. For each of the four experiments, the same pretrained architectures and feature extraction points have been used. This section details how feature extraction is performed from the different networks and why those particular extraction points were chosen. A summary of the pretrained networks used and at which points features are extracted is detailed in Table II.

The loss networks used for the experiments are created by selecting an architecture and a feature extraction point. A model of the selected architecture pretrained on ImageNet is then collected and layers after the extraction point are removed, and the output of the loss network is the features extracted at the selected point. How these features are used is described in the Experimental Details section.

As one of the objectives of this work is to evaluate where to perform feature extraction, the extraction points have been distributed throughout the network. Furthermore, the extraction points have been limited to the convolutional layers of the networks as these are typically used for deep perceptual loss. Additionally, the convolutional layers benefit from having no upper limit to the size of the input images, while using later layers typically requires the use of an exact input size.

Since testing all available extraction points would require a computation load that is unjustifiable for this work, four points were chosen for each network. The points were chosen such that they represent points that are early, semi-early, middle, and late in the convolutional layers. Additionally, for architectures of similar design, the extraction points are chosen such that they represent the "same" points in each network. For example, in the residual networks, the extraction points are after the first ReLU as well as after the same block stacks with the difference that each residual network architecture has a varying number of layers in the different block stacks.

IV. BENCHMARKS

In order to evaluate the effects of loss networks with different pretrained architectures and feature extraction points this work

TABLE I

Attributes of the ImageNet pretrained Torchvision [25] models used in this work. Shown are their accuracy on ImageNet, depth, MFLOPS for the forward pass (for a 224×224 pixel image), and whether the architecture has skip-connection, branches, 1×1 convolutions, or batch normalization.

Family	Architecture	ImageNet Acc. (%)	Depth	MFLOPS	Skip-conn.	Branch	1×1 conv.	Batch norm
VGG	VGG-11 [29]	69.020	11	7637				
	VGG-16 [29]	71.592	16	15517				
	VGG-16_bn [29]	73.360	16	15544				✓
	VGG-19 [29]	72.376	19	19682				
ResNet	ResNet-18 [30]	69.758	18	1827	✓			✓
	ResNet-50 [30]	76.130	50	4143	✓		✓	✓
	ResNeXt-50 32x4d [65]	77.618	50	4298	✓	✓	✓	✓
Inception	GoogLeNet [31]	69.778	22	1516		✓	✓	✓
	InceptionNet v3 [66]	77.294	49	2850		✓	✓	✓
EfficientNet	EfficientNet_B0 [67]	77.692	81	407	✓			✓
	EfficientNet_B7 [67]	78.642	271	5308	✓			✓
Misc.	AlexNet [28]	56.522	8	717				
	DenseNet-121 [68]	74.434	121	2899	✓		✓	✓
	SqueezeNet 1.1 [69]	58.178	18	360		✓	✓	

TABLE II
Loss Network Architectures and Feature Extraction Points

Architecture	Feature Extraction Points
<i>VGG Networks</i>	
VGG-11 [29]	1st, 2nd, 4th, and 8th ReLU
VGG-16 [29]	2nd, 4th, 7th, and 13th ReLU
VGG-16_bn [29]	2nd, 4th, 7th, and 13th ReLU
VGG-19 [29]	2nd, 4th, 8th, and 16th ReLU
<i>Residual Networks</i>	
ResNet-18 [30]	1st ReLU, 1st, 2nd, and 4th Block Stack
ResNet-50 [30]	1st ReLU, 1st, 2nd, and 4th Block Stack
ResNeXt-50 32x4d [65]	1st ReLU, 1st, 2nd, and 4th Block Stack
<i>Inception Networks</i>	
GoogLeNet [31]	1st BN, 1st, 3rd, and 9th Inception Module
InceptionNet v3 [66]	3rd BN, 1st, 3rd, and 8th Inception Module
<i>EfficientNet</i>	
EfficientNet_B0 [67]	1st SiLU, 1st, 4th, and 7th MBConv
EfficientNet_B7 [67]	1st SiLU, 1st, 4th, and 7th MBConv
<i>Uncategorized Networks</i>	
AlexNet [28]	1st, 2nd, 3rd, and 5th ReLU
DenseNet-121 [68]	1st ReLU, 1st, 2nd, and 4th Dense Block
SqueezeNet 1.1 [69]	1st ReLU, 1st, 4th, and 8th Fire Module

uses the experiments of four papers as benchmarks. The benchmark experiments are run with each of the loss networks and the performance scores of those experiments are collected. These scores are used to observe how different attributes of the loss networks affect the downstream performance across different tasks. These observations can be used as a starting point for an in-depth analysis of what attributes make a good loss network. `urllib.error.URLError: <urlopen error [Errno 111] Connection refused>` The four benchmarks are based on the experiments from *The Unreasonable Effectiveness of Deep Features as a Perceptual Metric* [5] (Benchmark 1),

Perceptual Losses for Real-Time Style Transfer and Super-Resolution [6] (Benchmark 2), *Beyond the Pixel-Wise Loss for Topology-Aware Delineation* [7] (Benchmark 3), and *Pretraining Image Encoders without Reconstruction via Feature Prediction Loss* [8] (Benchmark 4). The four benchmarks cover different applications of loss networks; perceptual similarity (Benchmark 1), super-resolution transformation (Benchmark 2), image segmentation (Benchmark 3), and autoencoding (Benchmark 4).

The specific experiments selected for the benchmarks were based on three criteria; (i) diversity of applications, (ii) ease of implementation, and (iii) popularity. The four benchmarks are taken from different categories of applications to give coverage of the diversity of the field; similarity metrics (Benchmark 1), image synthesis and transformation (Benchmark 2), pixel-labelling (Benchmark 3), and feature learning (Benchmark 4). All four works had preexisting implementations and were decided to be easy to adapt for the evaluation in this work. As some of the authors had worked with Benchmark 4 prior, this implementation was already well understood and adapted for these experiments. Benchmark 1 and 2 both have had a significant impact with citations in the thousands. While Benchmark 3 and 4 do not boast as many citations they have been referenced plenty, especially considering that they represent less popular application categories than the other two.

Each benchmark and the datasets and performance scores they use are detailed in the subsections below. For complete technical details on the benchmarks, it is recommended to read the original works. Some changes have been made to the benchmarks from the original experiments, which are also detailed in the subsections.

A. Benchmark 1: Perceptual Similarity

The Unreasonable Effectiveness of Deep Features as a Perceptual Metric [5] evaluates the use of deep features of

ImageNet [4] pretrained CNNs a image similarity metric. To achieve this it introduces the Berkeley-Adobe Perceptual Patch Similarity (BAPPS) dataset that collects human judgments of similarity on a host of distorted image patches. BAPPS is used to evaluate similarity metrics by measuring how closely they align with human judgments. The paper shows that ImageNet pretrained deep perceptual similarity metrics outperform unsupervised pretraining [72], semi-supervised pretraining [73, 74, 75, 76], and rule-based methods on perceptual similarity on BAPPS and come close to human performance without any task-specific training. It also shows that performance can be improved by specifically training the loss networks on BAPPS, though the performance is only slightly better than purely pretrained loss networks and the pretrained networks perform better on the types of distortions not included in the training data. The evaluation is carried out for three architectures; VGG-16, AlexNet, and SqueezeNet 1.1 with features extracted from multiple layers across the architectures.

The BAPPS dataset consists of 64×64 image patches from several sources [4, 77, 78, 79, 80, 81] along with versions of those patches that have been distorted by common image augmentations and algorithms such as autoencoding, super-resolution upscaling, frame interpolation, deblurring, and colorization. The BAPPS dataset is split into two parts; Two Alternative Forced Choice (2AFC) and Just Noticeable Differences (JND). The former consists of triplets with an image patch and two distorted versions of that image patch. Each 2AFC triplet is labeled by the fraction of human judges that considered each distorted version to be more similar to the original. The JND part consists of image pairs that are labeled by the fraction of human judges that considered the pair to be the same image after a brief viewing. During judgment collection, there were additional image pairs that were actually the same as well as completely different to make the task non-trivial. The 2AFC part is further split into training and test sets while JND is purely used for testing. For Benchmark 1 no training is performed so only the test sets are used.

Benchmark 1 consists of evaluating loss networks on the BAPPS dataset according to the procedure set out in the paper that introduced it. This follows the same general procedure as most deep perceptual loss implementations, except more architectures are considered and only a single extraction layer is used for each loss network. The deep features extracted from each loss network are used to calculate a similarity between two images x and x_0 according to Eq. 1, where z and z_0 are the channel-wise unit-normalized feature extractions from the loss network and w are the importance weights.

$$d(x, x_0) = \sum_n \frac{1}{H_n W_n} w_n \odot \|z_n - z_{0n}\|_2^2 \quad (1)$$

The performance scores for Benchmark 1 are the same as those used for the BAPPS dataset; the average 2AFC score and mAP% on the JND part. The 2AFC score for a single triplet is described in Eq. 2 similarity metric d , an image x , distorted versions x_0 and x_1 , and the fraction J of judgments

that consider x_1 more similar to x than x_0 .

$$2AFC(x, x_0, x_1, J) = \begin{cases} J, & \text{if } d(x, x_1) < d(x, x_0) \\ 1 - J, & \text{otherwise} \end{cases} \quad (2)$$

B. Benchmark 2: Super-resolution

Perceptual Losses for Real-Time Style Transfer and Super-Resolution [6] shows that deep perceptual loss can be used to improve the performance of super-resolution applications. This is shown by implementing an image transformation network consisting of five modified [82] residual blocks [30] and training that network with both pixel-wise and deep perceptual loss. The deep perceptual loss is implemented using an ImageNet pretrained VGG-16 network with several feature extraction points spread across the network. The deep perceptual loss is calculated according to Eq. 3, where x is the ground-truth image, \hat{x} the output of the transformation network, and $\phi_n(x)$ are the features at layer n of the loss network ϕ with input x .

$$L_{feat}^{\phi, n}(\hat{x}, x) = \frac{1}{C_n H_n W_n} \|\phi_n(\hat{x}) - \phi_n(x)\|_2^2 \quad (3)$$

The image transformation networks are trained on 288×288 image patches from the MS-COCO training set [83], a dataset of 300000 natural images used for object detection, dense pose estimation, keypoint detection, image captioning, and semantic, instance, and panoptic segmentation.. The networks are tested on the images in the Set5 [18], Set14 [19] and BSD100 [20] datasets. The three test sets are collections of high-quality images that have become standard for evaluation of super-resolution models [80]. Since the transformation networks are fully convolutional, they are applied to the full images of the test sets. The transformation networks are trained and tested for $\times 4$ and $\times 8$ upscaling. The input images are downsampled by applying Gaussian blur with $\sigma = 1.0$ and downsampling by the given factor with bicubic interpolation.

The test performance of the transformation networks are measured as the peak signal-to-noise ratio (PSNR) and SSIM [43] between the upsampled output images and the ground truth images. Additionally, a study was conducted where humans judged the quality of the $\times 4$ upsampled images. The deep perceptual loss trained networks outperformed the pixel-wise trained ones on PSNR and SSIM as well as the human judgements. Interestingly, deep perceptual loss was outperformed by a state-of-the-art model called SRCNN [84] on PSNR and SSIM but won with a large margin on the human judgments.

Benchmark 2 consists of the training of image transformation networks for $\times 4$ and $\times 8$ upscaling following the same procedure as the paper. Training is performed using 10K images randomly chosen from the MS-COCO 2014 training set using a specific seed for reproducibility purposes. The original paper performed training for 200K iterations, but it is unclear whether a validation step was performed and which model was finally used for inference. In the preliminary experiments, several architectures collapsed in the final epochs and produced black images. To avoid having a collapsed model, in the final experiments, the models are also trained for 200K iterations

with an additional validation step in every epoch to retain the best model according to the PSNR metric for 100 images from the MS-COCO 2014 validation set. As commonly used in super-resolution, the performance scores for Benchmark 2 are the PSNR and SSIM scores for the Set 5, Set 14, and BSD100 datasets, with $\times 4$ and $\times 8$ upscaling. Since the style-transfer applications in the original work does not have performance scores they have not been included in the benchmark.

C. Benchmark 3: Image Segmentation

Beyond the Pixel-Wise Loss for Topology-Aware Delineation [7] applies deep perceptual loss to the task of delineating curvilinear structures through semantic segmentation. This is done by training the U-net architecture [21] using a combination of pixel-wise BCE and deep perceptual loss according to Eq. 4, where x and y are the input image and ground truth segmentation map and μ is a scalar that is set to keep the two losses at the same order of magnitude.

$$L(x, y) = L_{bce}(x, y) + \mu L_{top}(x, y) \quad (4)$$

An ImageNet pretrained VGG-19 architecture with feature extraction at three different early layers as well as all three layers at the same time is used for the loss networks. The deep perceptual loss is calculated according to Eq. 5, where U is the U-net model being trained, and ϕ_n^m is m -th feature map in layer n of the loss network ϕ with extraction layers $n \in N$ with C_n channels of size $W_n \times H_n$.

$$L_{top}(x, y) = \sum_{n=1}^N \frac{1}{C_n H_n W_n} \sum_{m=1}^{C_n} \|\phi_n^m(y) - \phi_n^m(U(x))\|_2^2 \quad (5)$$

Both during training and testing the U-net is applied iteratively three times in order to improve the prediction. To achieve this the network is given both the input image and the output of the previous iteration as input. The data from the previous iteration is left blank for the first iteration.

In the original work, the method is evaluated on three datasets: Cracks [85], The Massachusetts Roads Dataset (MRD) [22], and the ISBI'12 challenge [86]. The evaluation scores used are completeness, correctness, and quality of delineation on the test sets as defined in [87]. Completeness quantifies the fraction of ground-truth objects that have been correctly delineated by the model and correctness measures the fraction of predicted objects that have a matching ground-truth object. The quality metric is a balance between the two by giving the fraction of all ground-truth and predicted objects that were correctly delineated. In short, completeness, correctness, and quality are analogs to recall, precision, and critical success index respectively. On all three datasets, it is shown that the addition of deep perceptual loss gives improved performance, both with and without iterative application.

Benchmark 3 only considers evaluation on MRD with input patches resized to 224×224 for computational efficiency. MRD is a set of 1171 aerial images with labeled by where the roads are as segmentation maps. In the original work, details of training epochs remain unclear, so all the benchmark is trained for 100 epochs as efficiency and computation trade-offs. The value of μ is also left ambiguous in the original work and has

been set to 0.01 for the benchmark. The performance scores for Benchmark 3 are the completeness, correctness, and quality on the MRD test set. Paper

D. Benchmark 4: Autoencoding

Pretraining Image Encoders without Reconstruction via Feature Prediction Loss [8] applies deep perceptual loss to autoencoder training for downstream prediction. The work shows that image autoencoders trained with deep perceptual loss learn more useful features for downstream prediction, than those trained with pixel-wise loss. This is achieved by adapting a previous image autoencoder setup [88], training it to encode and reproduce images, and training small Multi-Layer Perceptrons (MLP) on downstream tasks using the autoencoder embeddings as input. The performance of the downstream MLP reflects how useful the learned embeddings are for predictions and, therefore, which loss is best to use for training the autoencoders for downstream prediction.

The deep perceptual loss is calculated using features extracted from the second ReLU of an ImageNet pretrained AlexNet. The loss calculation for autoencoder training is described in Eq. 6, where x is the input image, $A(x)$ is the autoencoder reconstruction, ϕ a loss network with m extracted features.

$$L_{dp}(x) = \sum_{k=1}^m \|\phi(x)_k - \phi(A(x))_k\|_2^2 \quad (6)$$

The downstream tasks that the autoencoders are evaluated on are classification on the SVHN [23] and STL-10 [24] datasets, as well as object positioning on images gathered from the LunarLander-v2 environment of the OpenAI Gym [89]. For all three evaluations, the autoencoders are trained on an auxiliary set of images from the data, the MLPs are trained and validated on an 80/20 split of the training sets, and the MLPs for each autoencoder with the best validation score are tested on the test sets. The auxiliary images are those in the extra set from SVHN and the unlabeled images from STL-10.

For Benchmark 4 only the SVHN and STL-10 evaluations are performed. SVHN consists of 32×32 pixel images of house number digits that are labeled by the digit, which are scaled up to 64×64 images through reflection padding. STL-10 consists of 96×96 pixel images of animals and vehicles taken from ImageNet, where the training and test sets consist of 4 vehicle and 6 animal classes. The autoencoders have an embedding size of 64 and are trained for 10 epochs using the loss in Eq. 6 with the different loss networks. For each autoencoder, seven different MLPs with zero, one, and two hidden layers and various layer sizes are trained for 100 epochs each. The performance scores for the benchmark are the test set accuracies of the MLP with the best validation accuracy for each autoencoder on SVHN and STL-10.

The training epochs are reduced compared to the original work to save computation and it has been confirmed through smaller-scale experiments that this only minimally affects performance. The exclusion of the LunarLander-v2 evaluation was to save computation, because collecting the necessary data

is unwieldy, and since the environment has not been used in that way in other work.

V. RESULTS AND ANALYSIS

The performance scores on the four benchmarks have been analyzed together with a host of different attributes to attempt to provide insights into how to decide which architecture to choose and what layers to extract features from. The attributes that have been analyzed can be split into those that depend only on the architecture and those that depend on the architecture and extraction point. The attributes that depend on the architecture are, ImageNet accuracy, number of parameters, depth², flops in the forward pass, and whether the architectures uses skip-connections, branching, 1×1 -convolutions, or batch norm. The attributes that also depend on the extraction point are the number of parameters and depth before the extraction point as well as the number of features and channels at the extraction point. Additionally, some attributes derived from these were used, such as the fraction of the architecture’s total parameters that exist up until the extraction points. Finally, the performance scores of the four benchmarks were compared with each other to identify potential task-independent trends.

A large amount of data has been gathered from several evaluations over the four benchmarks, which is unwieldy to include in a paper in its entirety. For this reason, the raw data and attributes have been relegated to supplementary material for those that wish to make a deeper examination. More information about the supplementary material, including how to easily access the raw data and quickly generate scatterplots of attributes and performance scores can be found in the Appendix. This section presents the data of general interest such as indications of trends or lack thereof.

From the data gathered three primary findings related to how to select a loss network were identified. Those three findings are summarized below and then expanded on in their respective subsections.

- 1) In general, the VGG networks without batch norm and SqueezeNet perform well for most tasks if the correct layers are used.
- 2) Using the correct extraction point is at least as important as selecting the architecture.
- 3) There is no simple correlation between an architecture’s performance on ImageNet and its performance as a loss network.

Furthermore, some correlations which are typically assumed in the field of transfer learning were not observed. The analysis of the implications of these results is further expanded in the Discussion section.

A. Impact of architecture

To gain insight into what architecture attributes are beneficial for a loss network, the performance of each architecture is analyzed. In Table III, a summary of each architecture’s

²Depth is measured as the maximum number of non-linearly separated matrix multiplications up to the given point (*i.e.*, if the architecture branches and then rejoins only the longest branch is counted).

TABLE III
Rankings of the best loss network for each architecture on the performance scores averaged per benchmark

Architecture	Average ranking per benchmark				
	1	2	3	4	All
<i>VGG Networks</i>					
VGG-11 [29]	2.5	2.33	2.67	6	3.38
VGG-16 [29]	4.5	6.75	3.67	1.5	4.10
VGG-16_bn [29]	4.5	11.08	11.33	9.5	9.10
VGG-19 [29]	7	4.25	1.67	1.5	3.60
<i>Residual Networks</i>					
ResNet-18 [30]	5.5	7.08	12.67	8	8.31
ResNet-50 [30]	10	7.33	6.67	8.5	8.13
ResNeXt-50 32x4d [65]	11.5	5.67	5.67	9.5	8.08
<i>Inception Networks</i>					
GoogLeNet [31]	8.5	9.67	10.33	5.5	8.50
InceptionNet v3 [66]	10.5	11.83	4.67	11	9.50
<i>EfficientNet</i>					
EfficientNet_B0 [67]	9	9.92	11.67	8.5	9.77
EfficientNet_B7 [67]	12.5	8.83	3	8.5	8.21
<i>Uncategorized Networks</i>					
AlexNet [28]	5	8.58	9.33	10	8.23
DenseNet-121 [68]	10.5	10.5	13.67	8.5	10.79
SqueezeNet 1.1 [69]	3.5	1.17	8	8.5	5.29

performance is presented. For each performance score, the architectures are ranked according to the performance of the best extraction point between 1 (best) and 14 (worst). The table presents the average ranking of each architecture per benchmark as well as the overall average (each benchmark is weighted equally).

Across all four benchmarks two VGG networks without batch norm place in the top three when averaging the rankings of all performance scores (when the best extraction point is used for all networks). Interestingly the VGG-16 network with batch norm places in the bottom four on all benchmarks except perceptual similarity (Benchmark 1). The only network besides the VGG networks that do not use batch norm is AlexNet, which gets an average of 8th place over all four benchmarks. Another architecture that performs well is SqueezeNet which has an average performance on the delineation (Benchmark 3) and autoencoder training (Benchmark 4) scores but is second best at perceptual similarity (Benchmark 1) and the best at super-resolution (Benchmark 2). SqueezeNet is also a good option in all benchmarks when looking for performance as well as low computational needs. It is also worth noting that besides adding batch norm to VGG, the architectures within the same basic template (VGGs, ResNets, and EfficientNets) perform similarly, with little indication of which would be the better choice.

B. Impact of Extraction Point

The selection of where the features used for loss calculation are extracted in the network has a huge impact on the performance across all performance scores and architectures.

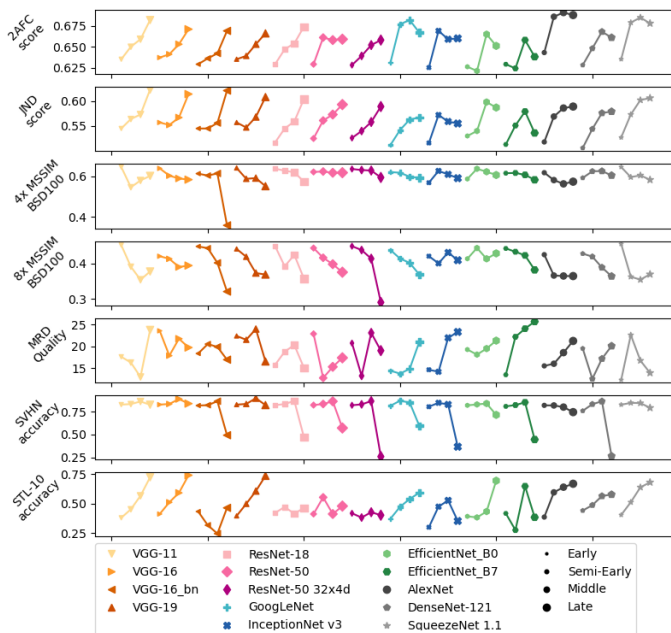


Fig. 2. The results of each loss network ordered by extraction point (earliest to latest) for some performance scores for each benchmark.

For all performance score, selecting the best extraction point of the worst architecture will give around the same performance as selecting the worst extraction point of the best architecture. This shows that selecting the extraction point for the loss network is as significant as selecting which model to use. In Table IV the best layer for each architecture is shown for some performance score of each benchmark. The architecture with the best performance for the performance score is underlined. In Figure 2 the performance of each architecture is shown for all their extraction points for some of the performance scores.

Interestingly, for most performance scores the extraction point which performs best is similar across architectures. This indicates that the selected extraction points are roughly equivalent which is desired and reinforces the existing consensus that two deep networks will learn similar features at similar points along their depth. However, the spread of which extraction points give the best performance on the different performance scores goes against the common practice of using the last or later layer for feature extraction. For a majority of architectures, the earliest extraction point is the best for the super-resolution experiments (Benchmark 2) on all performance scores, while the last extraction point gives the highest downstream accuracy on STL-10 (Benchmark 4).

So, while there exists some agreement between architectures as to which extraction point to use, that point depends on the task and dataset. While the gathered data does not give a conclusive way to predict which extraction point will be best for a given task and dataset, there are some trends.

Selecting an extraction point for a loss network determines what features will be compared during the calculation of loss or similarity. When optimizing the loss, the output will trend towards an image that gives rise to similar activations at the extraction point. Deeper layers of networks are known to

represent higher-level features, so the extraction point directly affects which type of features will be emphasized in image generation. Extracting from early layers means that the smaller pixel level patterns affect loss more while from later layers means that the general content and structure of the image affect the loss more. Whether it is best to optimize images on lower or higher-level features depends on the task. For example, in the super-resolution experiments (Benchmark 1) for all three test datasets, the optimal extraction point was early. Since super-resolution is a task where the individual pixels matter a lot, it is not unexpected that earlier extraction points that are focused on low-level features are best.

For the task of training an autoencoder for downstream predictions (Benchmark 4) later extraction points perform better. Likely this is due to classification tasks relying on higher-level features which means that autoencoders trained to replicate images that are similar in the later layers, would therefore also encode information relevant to higher-level features. The difference between the two evaluated datasets, SVHN and STL-10, is also noteworthy. For SVHN accuracy most architectures performed the best using the middle extraction point, compared to STL-10 accuracy for which the late extraction point was preferred. This difference is visualized in Fig. 3 which shows the performance of the different loss networks, grouped by extraction point, on the two datasets. This is notable since STL-10 is derived from a subset of ImageNet. SVHN on the other hand is the adjusted close-up images of house number digits, which are different from the typical photos in the ImageNet dataset. This also fits into the idea that the extraction point should match the task since the features in the later layers are expected to be more specific to the pretraining dataset and therefore more useful for extracting features of a similar dataset. When selecting an extraction point it is therefore worth considering how similar the dataset is to the one used for pretraining the loss networks.

Another consideration when selecting an extraction point (and architecture) is the computational demands during training. Some of the architectures that were evaluated require high amounts of computation on top of that required for the model that is being trained. For training smaller models this could potentially increase the computation power needed to train an order of magnitude. Using earlier extraction points means smaller loss networks, which reduce this additional computation. Taking into account that the later extraction points do not always perform better, this makes the argument for using earlier extraction points stronger. This is illustrated in Fig. 4 where, for each loss network, the 2AFC score is plotted against the \log_{10} amount flops for the forward pass. It is clear that selecting an earlier extraction point can potentially reduce the computation requirements by orders of magnitude.

C. Loss network performance vs. ImageNet accuracy

For the architectures and extraction points tested in this work there does not seem to be any strong correlation between the ImageNet accuracy of the loss network and the downstream performance of the models trained with them. The positive linear correlation between ImageNet accuracy and

TABLE IV

The feature extraction point with the best performance of each architecture for some performance scores of each benchmark. The letters indicate extraction points with the best loss network overall being underlined (E: Early, S: Semi-Early, M: Mid, L: Late).

Architecture	The best performing extraction point per performance score.						
	Benchmark 1		Benchmark 2		Benchmark 3	Benchmark 4	
	2AFC	JND	4x MSSIM BSDS100	8x MSSIM BSDS100	MRD (All)	SVHN	STL-10
<i>VGG Networks</i>							
VGG-11 [29]	L	<u>L</u>	<u>E</u>	E	L	M	L
VGG-16 [29]	L	L	E	E	E	M	<u>L</u>
VGG-16_bn [29]	L	L	M	E	S	M	L
VGG-19 [29]	L	L	E	E	<u>M</u>	<u>M</u>	L
<i>Residual Networks</i>							
ResNet-18 [30]	L	L	E	E	M	M	S
ResNet-50 [30]	S	L	S	E	E	M	S
ResNeXt-50 32x4d [65]	L	L	E	E	M	M	M
<i>Inception Networks</i>							
GoogLeNet [31]	M	L	E	E	L	S	L
InceptionNet v3 [66]	S	S	S	M	L	S	M
<i>EfficientNet</i>							
EfficientNet_B0 [67]	M	M	S	S	L	M	L
EfficientNet_B7 [67]	M	M	S	E	L	M	M
<i>Uncategorized Networks</i>							
AlexNet [28]	<u>M</u>	L	E	E	L	E	L
DenseNet-121 [68]	M	L	M	E	L	M	L
SqueezeNet 1.1 [69]	M	L	E	<u>E</u>	L	S	L

downstream performance that is often expected in computer vision transfer learning was absent in all performance scores. This has previously been shown to hold for deep perceptual similarity [41], and now also seems to hold for deep perceptual loss. However, the upper bound of perceptual similarity as a function of ImageNet performance that was reported in that work has not been replicated or refuted for deep perceptual loss. It would likely require an evaluation of orders of magnitude more loss network to do so. The performance of the best loss network for each architecture on MRD Quality compared to the ImageNet top-1 accuracy is shown in Fig. 5.

VI. DISCUSSION

The discussion of this work is divided into four subsections. The first suggests an approach to implementing a suitable loss network for a given task and dataset based on the findings in this work and others. The second discusses the the two transfer learning conventions that do not hold for deep perceptual loss and what this entails for the larger field. The third describes the limitation of this work and what weaknesses there may be in the findings. The final subsection suggests promising directions for future research, both regarding deep perceptual loss and the wider field of transfer learning.

A. Implementing a suitable loss network

This work evaluates 14 different ImageNet pretrained architectures with four different extraction points on four benchmarks. The results of this evaluation, combined with

results from previous works, provides insight into how to implement a suitable ImageNet pretrained loss network for a given task.

When it comes to the choice of architecture, the VGG networks without batch norm perform well on all four benchmarks. Out of them VGG-11 performs best on average, though both VGG-16 and 19 have benchmarks where they outperform the other VGG networks. While it may be interpreted that batch norm leads to poor performance it cannot be stated whether this generalizes beyond the VGG networks. Additionally, in Torchvision the models with batch-norm use a different pretraining procedure than those without, specifically they use a larger learning rate. This means that even if there was a clear difference between the architectures with and without batch-norm, this difference might be due to the training procedure rather than the architecture itself. SqueezeNet also performs well on Benchmark 1 and 2 which focus more on small scale features, especially super-resolution where focus on the large scale features are not as necessary as they are part of the input to the image transformation network. SqueezeNet has average performance on the remaining benchmarks. Despite these clear indicators of some architectures performing better, it is difficult to generalize there findings and point out which attributes of these networks make them perform well. There is no strong correlation in the gathered data between different architecture attributes and loss network performance. For most attributes this lack of correlation may be due to the size of the data, and studies targeting specific attributes may find those. Though, it seems clear from the data that the total depth and

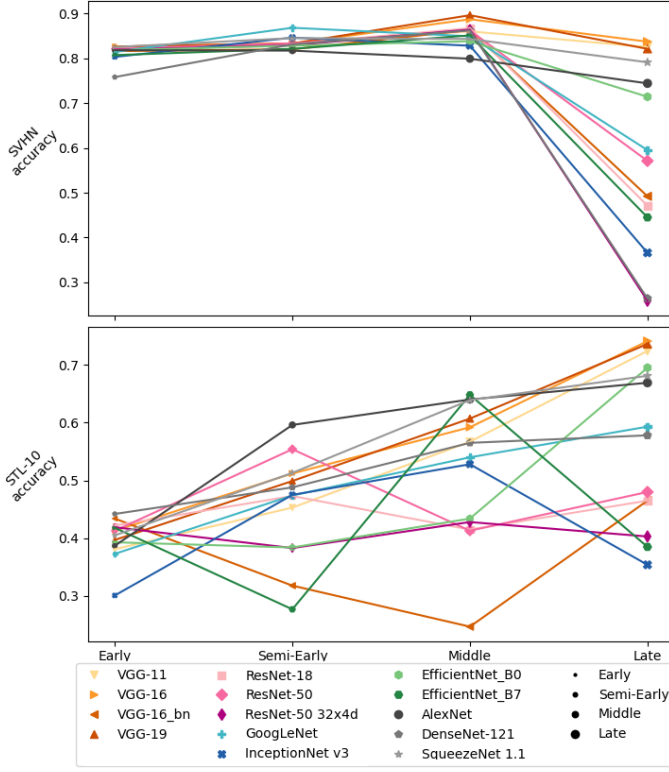


Fig. 3. The performance of all loss networks on SVHN and STL-10 where each loss network has been grouped by its extraction point. More figures like these can be quickly generated in the supplementary spreadsheet, using any combination of investigated attributes and performance scores.

number of parameters of a model does not affect its downstream performance as a loss network.

Some of the most novel finds of this work regards the choice of extraction point for deep features of the loss networks. The choice of feature extraction point has at least as much impact on loss network performance as the choice of pretrained architecture. It is also interesting to note that the extraction point that performs best on a performance score is correlated between different architectures. So if one architecture perform well on a task with a certain feature extraction point, it is likely that other architectures will perform, relatively, well on the task with feature extraction points at the similar relative depth. Though, the optimal feature extraction depth does not correlate between benchmarks, nor between tasks if the tasks are substantially different.

Some inference can be made as to which feature extraction points will perform well on a task based on the parameters of that task. Most performance scores on Benchmark 2 are improved for the earlier layers. One factor is that the performance is measured with scores focusing on low-level features, which likely align closer to the features detected by earlier layers. Another factor is that the input to the image transformation network contains the higher level structures, learning to replicate those structures should be easier as this can be achieved with the identity function, while the pixel-level differences are more difficult to learn. In such cases early layers perform better. If the performance scores are less dependent

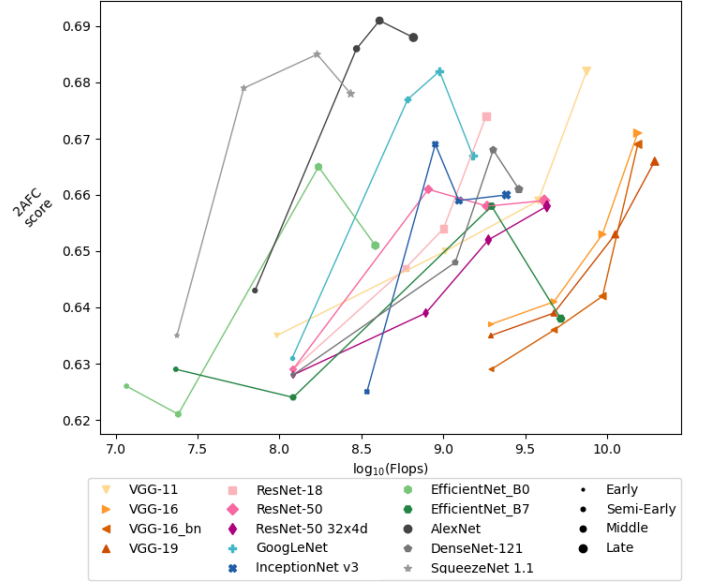


Fig. 4. The performance of all loss networks on the 2AFC split of BAPPS compared to the \log_{10} amount of flops in a forward pass of that loss network.

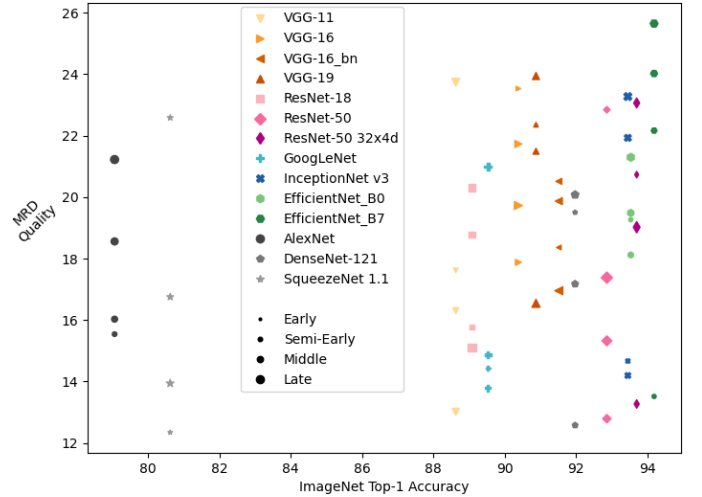


Fig. 5. The MRD Quality performance of each loss network compared to the ImageNet top-1 accuracy or the pretrained models.

on low-level structures, such as classification accuracy, or if the relevant high-level structures are not included in the input, such as image segments, later layers likely perform better. Additionally, how similar the pretraining data is to the task data likely also affect which extraction point is more suitable. Discussion This can be observed in Benchmark 4, where the later extraction points in general perform well on STL-10 which is derived from the pretraining dataset, while scores on SVHN, which is drawn from a substantially different distribution, are better for earlier extraction points. This is likely since the later layers have learned features that are specifically useful for the classes in ImageNet, and thus do not generalize well to SVHN.

An aspect that is not explored in this work is how the

loss network is pretrained. Kumar *et al.*, [41] showed that performance on BAPPS perceptual similarity dataset could be improved by pretraining models on ImageNet with other parameters and for fewer epochs than what would give optimal ImageNet accuracy. It is possible that such specialized pretraining could improve performance on deep perceptual loss tasks as well. Though, since deep perceptual loss tasks requires training another model with the loss network, such experiments would likely be prohibitively computationally expensive. Though additional pretraining on the distribution of the downstream task might lead to more suitable deep features in the later layers as was observed in Benchmark 4 with SVHN and STL-10 accuracy.

Another interesting finding is that, besides VGG networks generally performing well, the performance of a loss network on one benchmark does not predict its performance on another. This means that for a new task it can be difficult to predict which loss networks should perform well and likely several will have to be tested. If computation is limited, evaluating feature extraction points on VGG networks are recommended. If more computation is available it is also worth exploring some additional architectures with similar relative depth of the feature extraction points as the best performing VGG networks. As pretraining architectures can be orders of magnitude more expensive than evaluating them, this is only recommended in circumstances where resources are plentiful, slight gains in performance are important, and the model will be extensively used for inference.

There are other potential methods for implementing better performing loss networks that have not been analyzed in this work. Some of those methods are presented later in Subsection VI-D.

B. Breaking transfer learning conventions

The field of transfer learning have many conventions and accepted good practices. For some problems and conventions there is extensive empirical support, though the conventions are often followed beyond these cases. The results in this work shows that deep perceptual loss breaks two commonly held transfer learning conventions. First, it extends the findings on perceptual similarity by Kumar *et al.*, [41] that ImageNet accuracy is not positively correlated with downstream performance, to deep perceptual loss. Second, it demonstrates that for deep perceptual loss and similarity the later layers are not necessarily better for feature extraction. Both of these findings are expanded upon below.

In computer vision it is a common convention that improved ImageNet accuracy leads to better downstream performance on transfer learning tasks and this convention has been supported by trends [41] and specific studies [40] for some problems. However, on no benchmark can a positive correlation between the ImageNet accuracy of a model and its performance as a loss network be found. Kumar *et al.*, [41] also shows that downstream performance improves with ImageNet accuracy until some threshold accuracy after which downstream performance decreases as ImageNet accuracy increases. Though to find this correlation several thousands of loss networks were

examined. No such correlation could be found in the data gathered in this work, though likely if more loss networks were examined such patterns would reveal themselves. Another interesting point is that ImageNet accuracy is correlated with depth of the network, but this correlation cannot be found in the results of this work either. This lack of correlation with depth might be part of the reason why deep perceptual loss and similarity breaks this transfer learning convention. Especially, since it was also shown that the perceptual similarity scores of shallower architectures does not decay as much with increased ImageNet accuracy as their deeper counterparts [41].

In transfer learning in general it is also often held that the feature extraction should be performed in the later layers for better performance as these layers contain more advanced features [51].

C. Limitations of the study

The findings of this work are limited by a number of factors. The limited number of architectures tested is likely one of the reasons why no conclusion can be drawn relating to some attributes. The datasets used were mostly limited, especially within tasks, leading to the interpretations related to changing datasets being weak. The selected extraction points for each architecture are assumed to be equivalent, however, this might not be the case. Some architectures might perform worse simply due to the features at the selected extraction points being unsuitable for the tasks. However, in transfer learning settings it is commonly held that slight differences in extraction points only lead to minor changes in performance, especially if fine-tuning is used [50]. This reasoning might extend to deep perceptual loss as well, though further study would be needed.

Another potential problem with the work is the performance scores used in Benchmark 2. The performance scores, PSNR and SSIM, are the same as in the original work [6]. However, these metrics have been called into question when it comes to how well they represent the human perception of similarity [5]. This shortcoming is also noted in the original work, where their use is justified as a way to identify differences between losses rather than an attempt at showing state-of-the-art performance. In addition to this, it could be argued that performing well on both of these metrics might be a good indicator of quality even if it does not correlate directly with human perception of quality. Though, it is likely that the preference for earlier extraction points on Benchmark 2 is due to using performance scores that compare local and low-level features. The obvious alternatives to using such metrics would be to use deep perceptual similarity or human judgments, the former of which will bias the results towards the loss network chosen for similarity and the latter of which is expensive. Interestingly, there is no correlation between performance on the super-resolution subset of BAPPS and performance on the super-resolution metrics in Experiment 3, which seem to further indicate that the low-level metrics used do not correspond well to human perceptions of quality.

D. Future work

This work provides initial insight into how to implement suitable loss networks using pretrained architectures for a

given task. However, there are some parameters that were unexplored in this work, and of those that were explored more insight is needed. Additionally, more exploration of deep perceptual loss and similarity is needed, including studies that aggregate knowledge regarding the method. This work also has implications for the transfer learning field at large which suggests that further studies into other transfer learning applications are of interest. Below, these suggestions for future work are elaborated on.

While this work has shown that the popular VGG architectures are a good choice for loss networks, more data is needed to understand what attributes in general make an architecture perform well as a loss network. Ablation studies focusing on specific architecture attributes might provide further insight. However such studies would likely be computationally expensive in comparison to the usefulness of their findings, as which architectures perform well are not necessarily consistent between tasks. A more beneficial approach might be to find if performance on certain deep perceptual loss tasks is correlated with other tasks and if those tasks could be used as a proxy for evaluating loss networks.

The results of this work indicate that the optimal feature extraction point for deep perceptual loss and similarity can be predicted based on the task and pretraining data. Whether these indications hold on tasks and datasets beyond those evaluated in this work would require additional experiments. As is discussed below, such evaluations may be useful in the larger transfer learning domain.

Other important aspects of pretrained loss networks that are not covered by this work are the pretraining procedure and dataset. Kumar *et al.*, [41] showed that pretraining on ImageNet specifically for performance on perceptual similarity rather than accuracy can give significant improvement on perceptual similarity datasets. Though, attempting to explore the same for deep perceptual loss would likely be orders of magnitude more computationally expensive.

In the field of contrastive learning it has additionally been shown that ImageNet transfer learning is not as beneficial in image domains that are sufficiently different from natural scenes, such as medical images [90]. As a supplement, pretraining on images from the application domain is being investigated [90]. Such supplementary pretraining could likely benefit deep perceptual loss applications as well.

Beyond using pretrained loss networks, another common approach to deep perceptual loss is to train the loss network along with the network performing the task [10]. This is often done in a generative adversarial network setup where the discriminator is also used as a loss network. These methods are more difficult to evaluate and compare as they are typically designed to be task specific and would require extensive computation for a systematic evaluation as have been performed in this work.

A challenge for many of the presented directions of future analysis of loss networks is the computational demands needed for systematic evaluation. While the increasingly widespread use of deep perceptual loss might justify such studies, there are less demanding ways to aggregate knowledge of the method. As of yet no extensive survey covering either improvements

or applications of deep perceptual loss exists. Such a survey would likely be highly beneficial to the field as it could identify patterns of when the method performs better. Another strong benefit would be to unify the body of work and to spread insight between application areas which may otherwise be isolated from each other.

The findings of this work also suggest further work in the field of transfer learning. While it has been clearly demonstrated that increased ImageNet accuracy is correlated with increased performance for some cases [40, 41], it has also been shown that ImageNet pretraining is not as beneficial in other cases [91]. The Pareto front between ImageNet accuracy and perceptual similarity performance found by Kumar *et al.*, [41], likely exists for other tasks as well. It is well established in multi-task learning that a solution that is optimal for one task is rarely optimal for another [92]. As such Pareto front are likely to exist in most transfer learning settings. Studies probing when ImageNet pretraining is beneficial and at which accuracy the optimal downstream performance is reached would be beneficial to the field at large.

Another transfer learning convention in need of reevaluation is that the later layers are best suited for feature extraction. This work showed that this convention does not hold for deep perceptual loss and similarity. Likely this is the case for other transfer learning methods. Additionally, other findings relating to which layer is optimal and how the optimal layer correlates between layers might also generalize to the larger field of transfer learning. To investigate these conventions, surveys are likely a useful tool.

VII. CONCLUSION

Large-scale systematic testing and analysis of loss networks with varying architectures and extractions points have been performed. The results and analysis point to the three primary findings. First, selecting the extraction point for features is at least as important as selecting the architecture and good practice for making this selection is suggested. Secondly, while no general rule for selecting architecture could be identified, the VGG networks without batch norm are a good choice. Thirdly, there is no simple correlation between architecture attributes such as ImageNet accuracy, depth, and the number of parameters and downstream performance when used as a loss network.

The results also reinforce and expand earlier works showing that two established conventions within the field of transfer learning do not apply to deep perceptual loss and similarity. The conventions in question are that the final layers are the best candidates for feature extraction and that better ImageNet accuracy implies better downstream transfer learning performance. Further studies into these conventions and when they are applicable are needed,

ACKNOWLEDGMENT

This work required a lot of computation to complete, which was provided through the GPU data lab of Luleå University of Technology.

We would also like to thank Christian Günther for help with setting up the coding and execution environments that were used to implement many of the experiments.

REFERENCES

- [1] C. Szegedy, W. Zaremba, I. Sutskever, J. Bruna, D. Erhan, I. Goodfellow, and R. Fergus, “Intriguing properties of neural networks,” in *2nd International Conference on Learning Representations, ICLR*, 2014.
- [2] I. Goodfellow, J. Pouget-Abadie, M. Mirza, B. Xu, D. Warde-Farley, S. Ozair, A. Courville, and Y. Bengio, “Generative adversarial nets,” in *Advances in neural information processing systems*, 2014, pp. 2672–2680. [Online]. Available: <https://doi.org/10.1145/3422622>
- [3] J. Yosinski, J. Clune, A. M. Nguyen, T. J. Fuchs, and H. Lipson, “Understanding neural networks through deep visualization,” *arXiv preprint*, 2015.
- [4] J. Deng, W. Dong, R. Socher, L.-J. Li, K. Li, and L. Fei-Fei, “ImageNet: a large-scale hierarchical image database,” in *2009 IEEE Conference on Computer Vision and Pattern Recognition*, 2009, pp. 248–255.
- [5] R. Zhang, P. Isola, A. A. Efros, E. Shechtman, and O. Wang, “The unreasonable effectiveness of deep features as a perceptual metric,” in *Proceedings of the IEEE conference on computer vision and pattern recognition*, 2018, pp. 586–595.
- [6] J. Johnson, A. Alahi, and L. Fei-Fei, “Perceptual losses for real-time style transfer and super-resolution,” in *European conference on computer vision*. Springer, 2016, pp. 694–711. [Online]. Available: https://doi.org/10.1007/978-3-319-46475-6_43
- [7] A. Mosinska, P. Marquez-Neila, M. Koziński, and P. Fua, “Beyond the pixel-wise loss for topology-aware delineation,” in *Proceedings of the IEEE conference on computer vision and pattern recognition*, 2018, pp. 3136–3145.
- [8] G. G. Pihlgren, F. Sandin, and M. Liwicki, “Pretraining image encoders without reconstruction via feature prediction loss,” in *2020 25th International Conference on Pattern Recognition (ICPR)*, 2021, pp. 4105–4111.
- [9] L. A. Gatys, A. S. Ecker, and M. Bethge, “Image style transfer using convolutional neural networks,” in *Proceedings of the IEEE Conference on Computer Vision and Pattern Recognition (CVPR)*, June 2016.
- [10] A. B. L. Larsen, S. K. Sønderby, H. Larochelle, and O. Winther, “Autoencoding beyond pixels using a learned similarity metric,” in *Proceedings of The 33rd International Conference on Machine Learning*, ser. Proceedings of Machine Learning Research, vol. 48. PMLR, June 2016, pp. 1558–1566. [Online]. Available: <https://proceedings.mlr.press/v48/larsen16.html>
- [11] Q. Yang, P. Yan, Y. Zhang, H. Yu, Y. Shi, X. Mou, M. K. Kalra, Y. Zhang, L. Sun, and G. Wang, “Low-dose CT image denoising using a generative adversarial network with wasserstein distance and perceptual loss,” *IEEE Transactions on Medical Imaging*, vol. 37, no. 6, pp. 1348–1357, 2018.
- [12] Z. Chai, K. Zhou, J. Yang, Y. Ma, Z. Chen, S. Gao, and J. Liu, “Perceptual-assisted adversarial adaptation for choroid segmentation in optical coherence tomography,” in *2020 IEEE 17th International Symposium on Biomedical Imaging (ISBI)*, 2020, pp. 1966–1970.
- [13] G. G. Pihlgren, F. Sandin, and M. Liwicki, “Improving image autoencoder embeddings with perceptual loss,” in *2020 International Joint Conference on Neural Networks (IJCNN)*, 2020, pp. 1–7.
- [14] X. Liu, H. Gao, and X. Ma, “Perceptual losses for self-supervised depth estimation,” *Journal of Physics: Conference Series*, vol. 1952, no. 2, p. 022040, jun 2021. [Online]. Available: <https://dx.doi.org/10.1088/1742-6596/1952/2/022040>
- [15] K. Ding, K. Ma, S. Wang, and E. P. Simoncelli, “Image quality assessment: Unifying structure and texture similarity,” *IEEE Transactions on Pattern Analysis and Machine Intelligence*, vol. 44, no. 5, pp. 2567–2581, 2022.
- [16] A. Dosovitskiy and T. Brox, “Generating images with perceptual similarity metrics based on deep networks,” in *Advances in neural information processing systems*, 2016, pp. 658–666.
- [17] D. Xu, Y. Wang, X. Zhang, N. Zhang, and S. Yu, “Infrared and visible image fusion using a deep unsupervised framework with perceptual loss,” *IEEE Access*, vol. 8, pp. 206 445–206 458, 2020.
- [18] M. Bevilacqua, A. Roumy, C. Guillemot, and M.-L. Alberi-Morel, “Low-complexity single-image super-resolution based on nonnegative neighbor embedding,” in *BMVC*, 2012.
- [19] R. Zeyde, M. Elad, and M. Protter, “On single image scale-up using sparse-representations,” in *Curves and Surfaces*, 2010.
- [20] J.-B. Huang, A. Singh, and N. Ahuja, “Single image super-resolution from transformed self-exemplars,” *2015 IEEE Conference on Computer Vision and Pattern Recognition (CVPR)*, pp. 5197–5206, 2015.
- [21] O. Ronneberger, P. Fischer, and T. Brox, “U-net: Convolutional networks for biomedical image segmentation,” in *International Conference on Medical image computing and computer-assisted intervention*. Springer, 2015, pp. 234–241.
- [22] V. Mnih, “Machine learning for aerial image labeling,” Ph.D. dissertation, University of Toronto, 2013.
- [23] Y. Netzer, T. Wang, A. Coates, A. Bissacco, B. Wu, and A. Y. Ng, “Reading digits in natural images with unsupervised feature learning,” in *NIPS Workshop on Deep Learning and Unsupervised Feature Learning 2011*, 2011.
- [24] A. Coates, A. Ng, and H. Lee, “An analysis of single-layer networks in unsupervised feature learning,” in *Proceedings of the fourteenth international conference on artificial intelligence and statistics*, 2011, pp. 215–223.
- [25] S. Marcel and Y. Rodriguez, “Torchvision the machine-vision package of torch,” in *Proceedings of the 18th ACM International Conference on Multimedia*, ser. MM ’10. Association for Computing Machinery, 2010, p. 1485–1488. [Online]. Available: <https://doi.org/10.1145/>

- 1873951.1874254
- [26] A. Paszke, S. Gross, F. Massa, A. Lerer, J. Bradbury, G. Chanan, T. Killeen, Z. Lin, N. Gimelshein, L. Antiga, A. Desmaison, A. Kopf, E. Yang, Z. DeVito, M. Raison, A. Tejani, S. Chilamkurthy, B. Steiner, L. Fang, J. Bai, and S. Chintala, "PyTorch: an imperative style, high-performance deep learning library," in *Advances in Neural Information Processing Systems 32*, H. Wallach, H. Larochelle, A. Beygelzimer, F. d'Alché-Buc, E. Fox, and R. Garnett, Eds. Curran Associates, Inc., 2019, pp. 8024–8035.
 - [27] A. Krizhevsky, I. Sutskever, and G. E. Hinton, "ImageNet classification with deep convolutional neural networks," in *Advances in Neural Information Processing Systems 25*, F. Pereira, C. J. C. Burges, L. Bottou, and K. Q. Weinberger, Eds. Curran Associates, Inc., 2012, pp. 1097–1105.
 - [28] A. Krizhevsky, "One weird trick for parallelizing convolutional neural networks," *arXiv preprint*, 2014.
 - [29] K. Simonyan and A. Zisserman, "Very deep convolutional networks for large-scale image recognition," in *International Conference on Learning Representations*, 2015.
 - [30] K. He, X. Zhang, S. Ren, and J. Sun, "Deep residual learning for image recognition," in *2016 IEEE Conference on Computer Vision and Pattern Recognition (CVPR)*, 2016, pp. 770–778.
 - [31] C. Szegedy, Wei Liu, Yangqing Jia, P. Sermanet, S. Reed, D. Anguelov, D. Erhan, V. Vanhoucke, and A. Rabinovich, "Going deeper with convolutions," in *2015 IEEE Conference on Computer Vision and Pattern Recognition (CVPR)*, 2015, pp. 1–9.
 - [32] G. Farias, S. Dormido-Canto, J. Vega, G. Rattá, H. Vargas, G. Hermosilla, L. Alfaro, and A. Valencia, "Automatic feature extraction in large fusion databases by using deep learning approach," *Fusion Engineering and Design*, vol. 112, pp. 979–983, 2016.
 - [33] G. E. Hinton and R. R. Salakhutdinov, "Reducing the dimensionality of data with neural networks," *science*, vol. 313, no. 5786, pp. 504–507, 2006.
 - [34] Y. Bengio, P. Lamblin, D. Popovici, and H. Larochelle, "Greedy layer-wise training of deep networks," *Advances in neural information processing systems*, vol. 19, 2006.
 - [35] Q. V. Le, "Building high-level features using large scale unsupervised learning," in *2013 IEEE international conference on acoustics, speech and signal processing*. IEEE, 2013, pp. 8595–8598.
 - [36] Y. Hayakawa, T. Oonuma, H. Kobayashi, A. Takahashi, S. Chiba, and N. M. Fujiki, "Feature extraction of video using deep neural network," in *2016 IEEE 15th International Conference on Cognitive Informatics & Cognitive Computing (ICCI* CC)*. IEEE, 2016, pp. 465–470.
 - [37] S. H. Lee, C. S. Chan, S. J. Mayo, and P. Remagnino, "How deep learning extracts and learns leaf features for plant classification," *Pattern Recognition*, vol. 71, pp. 1–13, 2017.
 - [38] B. Jiang, J. Yang, Z. Lv, K. Tian, Q. Meng, and Y. Yan, "Internet cross-media retrieval based on deep learning," *Journal of Visual Communication and Image Representation*, vol. 48, pp. 356–366, 2017.
 - [39] H. Mohsen, E.-S. A. El-Dahshan, E.-S. M. El-Horbaty, and A.-B. M. Salem, "Classification using deep learning neural networks for brain tumors," *Future Computing and Informatics Journal*, vol. 3, no. 1, pp. 68–71, 2018.
 - [40] S. Kornblith, J. Shlens, and Q. V. Le, "Do better imagenet models transfer better?" in *Proceedings of the IEEE/CVF Conference on Computer Vision and Pattern Recognition (CVPR)*, June 2019.
 - [41] M. Kumar, N. Houlsby, N. Kalchbrenner, and E. D. Cubuk, "Do better imagenet classifiers assess perceptual similarity better?" *Transactions on Machine Learning Research*, 2022.
 - [42] M. Alberti, M. Seuret, R. Ingold, and M. Liwicki, "A pitfall of unsupervised pre-training," *arXiv preprint*, 2017.
 - [43] Z. Wang, A. Bovik, H. Sheikh, and E. Simoncelli, "Image quality assessment: from error visibility to structural similarity," *IEEE Transactions on Image Processing*, vol. 13, no. 4, pp. 600–612, 2004.
 - [44] A. Babenko, A. Slesarev, A. Chigorin, and V. Lempitsky, "Neural codes for image retrieval," in *Computer Vision – ECCV 2014*. Springer International Publishing, 2014, pp. 584–599.
 - [45] M. Kettunen, E. Härkönen, and J. Lehtinen, "E-LPIPS: robust perceptual image similarity via random transformation ensembles," *arXiv preprint*, 2019.
 - [46] H. Zhao, O. Gallo, I. Frosio, and J. Kautz, "Loss functions for image restoration with neural networks," *IEEE Transactions on Computational Imaging*, vol. 3, no. 1, pp. 47–57, 2017.
 - [47] J. Snell, K. Ridgeway, R. Liao, B. D. Roads, M. C. Mozer, and R. S. Zemel, "Learning to generate images with perceptual similarity metrics," in *2017 IEEE International Conference on Image Processing (ICIP)*, 2017, pp. 4277–4281.
 - [48] K. Simonyan, A. Vedaldi, and A. Zisserman, "Deep inside convolutional networks: Visualising image classification models and saliency maps," in *Workshop at International Conference on Learning Representations*, 2014.
 - [49] J. Li, X. Liang, Y. Wei, T. Xu, J. Feng, and S. Yan, "Perceptual generative adversarial networks for small object detection," in *The IEEE Conference on Computer Vision and Pattern Recognition (CVPR)*, July 2017.
 - [50] J. Yosinski, J. Clune, Y. Bengio, and H. Lipson, "How transferable are features in deep neural networks?" *Advances in neural information processing systems*, vol. 27, 2014.
 - [51] F. Zhuang, Z. Qi, K. Duan, D. Xi, Y. Zhu, H. Zhu, H. Xiong, and Q. He, "A comprehensive survey on transfer learning," *Proceedings of the IEEE*, vol. 109, no. 1, pp. 43–76, 2021.
 - [52] C. Ledig, L. Theis, F. Huszár, J. Caballero, A. Cunningham, A. Acosta, A. Aitken, A. Tejani, J. Totz, Z. Wang et al., "Photo-realistic single image super-resolution using a generative adversarial network," in *Proceedings of the IEEE conference on computer vision and pattern recognition*, 2017, pp. 4681–4690.

- [53] C. Shi and C.-M. Pun, "Adaptive multi-scale deep neural networks with perceptual loss for panchromatic and multispectral images classification," *Information Sciences*, vol. 490, pp. 1–17, 2019.
- [54] P. Rasti, T. Uiboupin, S. Escalera, and G. Anbarjafari, "Convolutional neural network super resolution for face recognition in surveillance monitoring," in *Articulated Motion and Deformable Objects*, F. J. Perales and J. Kittler, Eds. Cham: Springer International Publishing, 2016, pp. 175–184.
- [55] H. Greenspan, "Super-Resolution in Medical Imaging," *The Computer Journal*, vol. 52, no. 1, pp. 43–63, 2009.
- [56] J. S. Isaac and R. Kulkarni, "Super resolution techniques for medical image processing," in *2015 International Conference on Technologies for Sustainable Development (ICTSD)*, 2015, pp. 1–6.
- [57] Z. Wang, J. Chen, and S. C. H. Hoi, "Deep learning for image super-resolution: A survey," *IEEE Transactions on Pattern Analysis and Machine Intelligence*, vol. 43, pp. 3365–3387, 2021.
- [58] D. Dai, Y. Wang, Y. Chen, and L. Van Gool, "Is image super-resolution helpful for other vision tasks?" in *2016 IEEE Winter Conference on Applications of Computer Vision (WACV)*. IEEE, 2016, pp. 1–9.
- [59] K. He, G. Gkioxari, P. Dollár, and R. Girshick, "Mask r-cnn," in *2017 IEEE International Conference on Computer Vision (ICCV)*, 2017, pp. 2980–2988.
- [60] Z. Zhang, P. Luo, C. C. Loy, and X. Tang, "Facial landmark detection by deep multi-task learning," in *Computer Vision—ECCV 2014: 13th European Conference, Zurich, Switzerland, September 6–12, 2014, Proceedings, Part VI 13*. Springer, 2014, pp. 94–108.
- [61] M. S. Rad, B. Bozorgtabar, U.-V. Marti, M. Basler, H. K. Ekenel, and J.-P. Thiran, "SROBB: targeted perceptual loss for single image super-resolution," in *Proceedings of the IEEE/CVF International Conference on Computer Vision (ICCV)*, October 2019.
- [62] D. E. Rumelhart, G. E. Hinton, and R. J. Williams, "Learning internal representations by error propagation," California Univ San Diego La Jolla Inst for Cognitive Science, Tech. Rep., 1985.
- [63] D. H. Ballard, "Modular learning in neural networks," in *AAAI*, 1987, pp. 279–284.
- [64] D. P. Kingma and M. Welling, "Auto-encoding variational bayes," *arXiv preprint*, 2013.
- [65] S. Xie, R. Girshick, P. Dollár, Z. Tu, and K. He, "Aggregated residual transformations for deep neural networks," in *Proceedings of the IEEE conference on computer vision and pattern recognition*, 2017, pp. 1492–1500.
- [66] C. Szegedy, V. Vanhoucke, S. Ioffe, J. Shlens, and Z. Wojna, "Rethinking the inception architecture for computer vision," in *2016 IEEE Conference on Computer Vision and Pattern Recognition (CVPR)*, 2016, pp. 2818–2826.
- [67] M. Tan and Q. Le, "Efficientnet: Rethinking model scaling for convolutional neural networks," in *International Conference on Machine Learning*. PMLR, 2019, pp. 6105–6114.
- [68] G. Huang, Z. Liu, L. Van Der Maaten, and K. Q. Weinberger, "Densely connected convolutional networks," in *2017 IEEE Conference on Computer Vision and Pattern Recognition (CVPR)*, 2017, pp. 2261–2269.
- [69] F. N. Iandola, S. Han, M. W. Moskewicz, K. Ashraf, W. J. Dally, and K. Keutzer, "SqueezeNet: AlexNet-level accuracy with 50x fewer parameters and <0.5MB model size," *arXiv preprint*, 2016.
- [70] K. De and M. Pedersen, "Impact of colour on robustness of deep neural networks," in *Proceedings of the IEEE/CVF International Conference on Computer Vision*, 2021, pp. 21–30.
- [71] B. Zoph and Q. Le, "Neural architecture search with reinforcement learning," in *5th International Conference on Learning Representations, ICLR*, 2017.
- [72] P. Krähenbühl, C. Doersch, J. Donahue, and T. Darrell, "Data-dependent initializations of convolutional neural networks," in *4th International Conference on Learning Representations, ICLR*, 2016.
- [73] D. Pathak, R. Girshick, P. Dollar, T. Darrell, and B. Hariharan, "Learning features by watching objects move," in *Proceedings of the IEEE Conference on Computer Vision and Pattern Recognition (CVPR)*, July 2017.
- [74] R. Zhang, P. Isola, and A. A. Efros, "Split-brain autoencoders: Unsupervised learning by cross-channel prediction," in *Proceedings of the IEEE Conference on Computer Vision and Pattern Recognition*, 2017, pp. 1058–1067.
- [75] M. Noroozi and P. Favaro, "Unsupervised learning of visual representations by solving jigsaw puzzles," in *European conference on computer vision*. Springer, 2016, pp. 69–84.
- [76] J. Donahue, P. Krähenbühl, and T. Darrell, "Adversarial feature learning," in *5th International Conference on Learning Representations, ICLR*, 2016.
- [77] D. Scharstein, R. Szeliski, and R. Zabih, "A taxonomy and evaluation of dense two-frame stereo correspondence algorithms," in *Proceedings IEEE Workshop on Stereo and Multi-Baseline Vision (SMBV 2001)*, 2001, pp. 131–140.
- [78] V. Bychkovsky, S. Paris, E. Chan, and F. Durand, "Learning photographic global tonal adjustment with a database of input/output image pairs," in *CVPR 2011*. IEEE, 2011, pp. 97–104.
- [79] D.-T. Dang-Nguyen, C. Pasquini, V. Conotter, and G. Boato, "Raise: A raw images dataset for digital image forensics," in *Proceedings of the 6th ACM multimedia systems conference*, 2015, pp. 219–224.
- [80] E. Agustsson and R. Timofte, "NTIRE 2017 challenge on single image super-resolution: Dataset and study," in *2017 IEEE Conference on Computer Vision and Pattern Recognition Workshops (CVPRW)*, 2017, pp. 1122–1131.
- [81] S. Su, M. Delbracio, J. Wang, G. Sapiro, W. Heidrich, and O. Wang, "Deep video deblurring for hand-held cameras," in *2017 IEEE Conference on Computer Vision and Pattern Recognition (CVPR)*, 2017, pp. 237–246.
- [82] S. Gross and M. Wilber, "Training and investigating residual nets," *Facebook AI Research*, vol. 6, no. 3,

2016. [Online]. Available: <http://torch.ch/blog/2016/02/04/resnets.html>
- [83] T.-Y. Lin, M. Maire, S. J. Belongie, J. Hays, P. Perona, D. Ramanan, P. Dollár, and C. L. Zitnick, “Microsoft COCO: common objects in context,” in *ECCV*, 2014.
 - [84] C. Dong, C. C. Loy, K. He, and X. Tang, “Image super-resolution using deep convolutional networks,” *IEEE transactions on pattern analysis and machine intelligence*, vol. 38, no. 2, pp. 295–307, 2015.
 - [85] Q. Zou, Y. Cao, Q. Li, Q. Mao, and S. Wang, “CrackTree: automatic crack detection from pavement images,” *Pattern Recognition Letters*, vol. 33, no. 3, pp. 227–238, 2012.
 - [86] I. Arganda-Carreras, S. C. Turaga, D. R. Berger, D. Cireşan, A. Giusti, L. M. Gambardella, J. Schmidhuber, D. Laptev, S. Dwivedi, J. M. Buhmann *et al.*, “Crowd-sourcing the creation of image segmentation algorithms for connectomics,” *Frontiers in neuroanatomy*, p. 142, 2015.
 - [87] C. Wiedemann, C. Heipke, H. Mayer, and O. Jamet, “Empirical evaluation of automatically extracted road axes,” *Empirical evaluation techniques in computer vision*, vol. 12, pp. 172–187, 1998.
 - [88] D. Ha and J. Schmidhuber, “Recurrent world models facilitate policy evolution,” in *Advances in Neural Information Processing Systems 31*, S. Bengio, H. Wallach, H. Larochelle, K. Grauman, N. Cesa-Bianchi, and R. Garnett, Eds. Curran Associates, Inc., 2018, pp. 2450–2462. [Online]. Available: <http://papers.nips.cc/paper/7512-recurrent-world-models-facilitate-policy-evolution.pdf>
 - [89] G. Brockman, V. Cheung, L. Pettersson, J. Schneider, J. Schulman, J. Tang, and W. Zaremba, “OpenAI gym,” *arXiv preprint*, 2016.
 - [90] P. Chandra Chhipa, “Self-supervised representation learning for visual domains beyond natural scenes,” Licentiate Thesis, Luleå tekniska universitet, 2023.
 - [91] M. Raghu, C. Zhang, J. Kleinberg, and S. Bengio, “Transfusion: Understanding transfer learning for medical imaging,” *Advances in neural information processing systems*, vol. 32, 2019.
 - [92] P. Ma, T. Du, and W. Matusik, “Efficient continuous pareto exploration in multi-task learning,” in *Proceedings of the 37th International Conference on Machine Learning*, ser. Proceedings of Machine Learning Research, vol. 119. PMLR, 13–18 Jul 2020, pp. 6522–6531.

APPENDIX

A. Overview of the Supplementary Material

A lot of data was gathered and aggregated for this work, too much to fit in the paper. Instead, this data is made available as supplementary material. The supplementary material is available in three different versions: An online spreadsheet³, three ancillary .csv files published alongside this work, and this appendix.

Each version of the supplementary material serves a different purpose. The online spreadsheet contains the raw attributes and performance scores as well as the derived attributes, aggregated results, and automatic generation of scatterplots similar to those found in this work. This facilitates quick access to and analysis of the data for the readers. The ancillary files contain the same raw data and derived attributes as the spreadsheet and are meant to guarantee that the raw data is available even if the online spreadsheet at some point becomes unavailable. The appendix contains the raw performance scores of the four benchmarks so that they may be easily accessible while reading.

The performance scores for the different architectures and extraction points for each of the four benchmarks are available in the following tables: Table V (Benchmark 1), Tables VI–IX (Benchmark 2), Table X (Benchmark 3), and Table XI (Benchmark 4).

TABLE V
2AFC and JND scores of the BAPPS dataset for different loss networks used to measure deep perceptual similarity

Architecture	2AFC score				JND score			
	E	S	M	L	E	S	M	L
<i>VGG Networks</i>								
VGG-11	0.635	0.650	0.659	0.682	0.545	0.564	0.573	0.623
VGG-16	0.637	0.641	0.653	0.671	0.557	0.552	0.567	0.614
VGG-16_bn	0.629	0.636	0.642	0.669	0.545	0.545	0.556	0.621
VGG-19	0.635	0.639	0.653	0.666	0.557	0.547	0.568	0.608
<i>Residual Networks</i>								
ResNet-18	0.629	0.647	0.654	0.674	0.517	0.545	0.559	0.604
ResNet-50	0.629	0.661	0.658	0.659	0.525	0.561	0.573	0.593
ResNeXt-50 32x4d	0.628	0.639	0.652	0.658	0.526	0.540	0.558	0.589
<i>Inception Networks</i>								
GoogLeNet	0.631	0.677	0.682	0.667	0.512	0.542	0.563	0.567
InceptionNet v3	0.625	0.669	0.659	0.660	0.516	0.572	0.559	0.555
<i>EfficientNet</i>								
EfficientNet_B0	0.626	0.621	0.665	0.651	0.530	0.540	0.598	0.587
EfficientNet_B7	0.629	0.624	0.658	0.638	0.513	0.551	0.579	0.536
<i>Uncategorized Networks</i>								
AlexNet	0.643	0.686	0.691	0.688	0.518	0.569	0.586	0.589
DenseNet-121	0.628	0.648	0.668	0.661	0.506	0.544	0.576	0.579
SqueezeNet	0.635	0.679	0.685	0.678	0.527	0.573	0.602	0.606

³bit.ly/loss-network-analysis

TABLE VI
PSNR of $\times 4$ upscaling on Set 5, Set 14, and BSD100 of an Image Transformation Network trained with different loss networks

Architecture	Set 5				Set 14				BSD100			
	E	S	M	L	E	S	M	L	E	S	M	L
<i>VGG Networks</i>												
VGG-11	30.7	28.6	28.1	27.2	26.4	24.9	24.7	24.7	26.3	24.9	24.7	25.2
VGG-16	30.3	27.2	24.9	25.5	26.3	24.7	23.7	24.1	25.9	24.9	23.8	23.9
VGG-16_bn	28.6	28.5	23.2	13.2	24.7	24.5	21.9	14.3	25.2	24.4	22.7	15.4
VGG-19	30.2	26.1	26.2	26.8	26.3	24.1	24.0	24.0	26.1	24.3	24.2	23.5
<i>Residual Networks</i>												
ResNet-18	28.7	26.8	28.3	25.5	25.4	24.1	24.8	23.1	25.9	24.5	24.6	23.6
ResNet-50	29.1	31.0	28.4	24.1	25.5	25.7	25.0	22.5	25.4	25.2	24.8	24.5
ResNeXt-50 32x4d	29.8	27.3	29.5	24.7	25.9	24.7	25.1	22.4	26.0	25.1	25.3	22.7
<i>Inception Networks</i>												
GoogLeNet	26.5	29.5	28.4	26.0	24.2	25.3	24.7	23.5	24.7	25.0	24.9	24.6
InceptionNet v3	27.4	27.4	26.3	24.9	24.2	24.7	24.0	23.7	24.5	25.4	24.0	24.0
<i>EfficientNet</i>												
EfficientNet_B0	21.1	26.8	27.3	25.8	20.7	24.5	24.3	24.1	21.1	25.0	24.8	24.5
EfficientNet_B7	28.6	27.7	27.9	26.1	25.5	24.8	24.6	23.4	25.6	25.8	24.9	23.5
<i>Uncategorized Networks</i>												
AlexNet	29.9	29.2	30.0	29.7	25.7	24.9	25.2	25.2	25.7	25.1	24.9	24.9
DenseNet-121	24.8	30.1	29.3	25.1	23.4	25.2	25.2	22.4	24.0	24.9	24.9	24.5
SqueezeNet	31.1	29.1	28.4	26.9	26.5	25.0	24.8	23.9	26.2	25.3	24.6	24.1

TABLE VII
MSSIM of $\times 4$ upscaling on Set 5, Set 14, and BSD100 of an Image Transformation Network trained with different loss networks

Architecture	Set 5				Set 14				BSD100			
	E	S	M	L	E	S	M	L	E	S	M	L
<i>VGG Networks</i>												
VGG-11	0.855	0.772	0.812	0.793	0.690	0.603	0.630	0.643	0.646	0.546	0.579	0.602
VGG-16	0.859	0.824	0.806	0.804	0.689	0.649	0.640	0.643	0.639	0.603	0.589	0.583
VGG-16_bn	0.834	0.832	0.807	0.382	0.664	0.660	0.653	0.318	0.613	0.604	0.614	0.357
VGG-19	0.856	0.809	0.815	0.803	0.693	0.641	0.639	0.625	0.641	0.587	0.591	0.551
<i>Residual Networks</i>												
ResNet-18	0.826	0.838	0.834	0.805	0.672	0.665	0.669	0.629	0.638	0.628	0.619	0.574
ResNet-50	0.835	0.856	0.837	0.742	0.671	0.677	0.668	0.619	0.621	0.623	0.617	0.618
ResNeXt-50 32x4d	0.840	0.836	0.846	0.824	0.678	0.671	0.673	0.647	0.636	0.631	0.628	0.594
<i>Inception Networks</i>												
GoogLeNet	0.822	0.847	0.832	0.773	0.655	0.670	0.651	0.615	0.621	0.618	0.598	0.592
InceptionNet v3	0.786	0.825	0.813	0.779	0.615	0.667	0.653	0.627	0.568	0.626	0.609	0.590
<i>EfficientNet</i>												
EfficientNet_B0	0.749	0.815	0.826	0.808	0.617	0.668	0.663	0.649	0.587	0.637	0.622	0.606
EfficientNet_B7	0.826	0.803	0.812	0.797	0.663	0.648	0.648	0.629	0.615	0.616	0.607	0.582
<i>Uncategorized Networks</i>												
AlexNet	0.828	0.803	0.815	0.814	0.665	0.627	0.624	0.632	0.618	0.581	0.562	0.573
DenseNet-121	0.784	0.851	0.845	0.777	0.628	0.678	0.674	0.624	0.592	0.625	0.626	0.604
SqueezeNet	0.861	0.816	0.831	0.808	0.693	0.641	0.655	0.637	0.646	0.596	0.605	0.582

TABLE VIII
PSNR of $\times 8$ upscaling on Set 5, Set 14, and BSD100 of an Image Transformation Network trained with different loss networks

Architecture	Set 5				Set 14				BSD100			
	E	S	M	L	E	S	M	L	E	S	M	L
<i>VGG Networks</i>												
VGG-11	26.2	26.0	22.8	19.6	22.8	22.5	20.9	18.4	22.6	22.1	21.3	19.0
VGG-16	25.2	23.4	19.9	18.6	22.5	21.4	19.5	19.0	22.3	21.5	20.1	19.7
VGG-16_bn	24.6	21.6	13.2	12.0	21.6	20.0	13.0	11.9	21.3	20.1	13.9	12.8
VGG-19	25.4	22.5	19.7	20.0	22.6	21.0	19.3	19.1	22.5	21.3	20.0	19.4
<i>Residual Networks</i>												
ResNet-18	25.6	24.9	23.2	22.1	22.4	21.8	20.5	20.3	22.3	21.5	20.7	20.9
ResNet-50	24.7	25.3	25.1	23.3	21.9	21.7	21.6	21.0	22.1	21.3	21.3	21.3
ResNeXt-50 32x4d	25.5	25.3	25.0	14.7	22.4	21.9	21.5	15.7	22.3	21.7	21.2	16.2
<i>Inception Networks</i>												
GoogLeNet	22.0	25.7	25.2	24.1	20.9	21.9	21.7	21.3	21.2	21.5	21.5	21.1
InceptionNet v3	22.6	24.2	23.8	24.5	20.7	21.7	21.7	21.9	21.3	21.7	21.7	21.8
<i>EfficientNet</i>												
EfficientNet_B0	18.4	24.4	25.4	24.8	18.8	22.0	22.2	22.0	19.3	22.2	21.9	21.8
EfficientNet_B7	25.0	23.5	25.8	24.6	22.2	21.3	22.4	21.8	22.4	21.9	22.2	22.0
<i>Uncategorized Networks</i>												
AlexNet	26.3	25.8	25.5	24.2	22.6	21.9	21.9	21.4	22.1	21.5	21.6	21.4
DenseNet-121	21.4	24.1	24.9	23.9	20.8	21.6	21.9	21.3	21.4	21.8	21.5	21.4
SqueezeNet	26.5	25.0	23.8	22.1	22.9	22.0	21.5	20.6	22.6	21.7	21.0	20.4

TABLE IX
MSSIM of $\times 8$ upscaling on Set 5, Set 14, and BSD100 of an Image Transformation Network trained with different loss networks

Architecture	Set 5				Set 14				BSD100			
	E	S	M	L	E	S	M	L	E	S	M	L
<i>VGG Networks</i>												
VGG-11	0.709	0.675	0.590	0.604	0.487	0.452	0.389	0.413	0.452	0.391	0.354	0.377
VGG-16	0.673	0.666	0.605	0.569	0.463	0.453	0.417	0.420	0.420	0.413	0.390	0.394
VGG-16_bn	0.685	0.649	0.518	0.380	0.478	0.458	0.385	0.282	0.448	0.443	0.401	0.321
VGG-19	0.696	0.661	0.591	0.574	0.481	0.450	0.402	0.399	0.441	0.419	0.373	0.369
<i>Residual Networks</i>												
ResNet-18	0.685	0.657	0.673	0.532	0.480	0.446	0.465	0.374	0.449	0.392	0.424	0.357
ResNet-50	0.678	0.688	0.685	0.588	0.479	0.464	0.456	0.402	0.443	0.416	0.398	0.375
ResNeXt-50 32x4d	0.696	0.695	0.690	0.341	0.483	0.476	0.468	0.272	0.449	0.438	0.413	0.290
<i>Inception Networks</i>												
GoogLeNet	0.617	0.695	0.673	0.620	0.454	0.459	0.460	0.427	0.438	0.414	0.401	0.369
InceptionNet v3	0.634	0.661	0.656	0.628	0.451	0.448	0.462	0.437	0.420	0.400	0.431	0.409
<i>EfficientNet</i>												
EfficientNet_B0	0.592	0.669	0.688	0.667	0.436	0.469	0.466	0.460	0.413	0.443	0.413	0.428
EfficientNet_B7	0.674	0.644	0.662	0.599	0.470	0.447	0.467	0.409	0.442	0.433	0.423	0.382
<i>Uncategorized Networks</i>												
AlexNet	0.681	0.636	0.631	0.611	0.469	0.413	0.412	0.406	0.425	0.366	0.364	0.364
DenseNet-121	0.605	0.648	0.650	0.582	0.438	0.459	0.436	0.398	0.428	0.419	0.388	0.364
SqueezeNet	0.710	0.606	0.627	0.611	0.491	0.406	0.417	0.417	0.455	0.362	0.354	0.369

TABLE X
Correctness, Completeness, and Quality on the MRD testset for U-net models trained with different loss networks

Architecture	Correctness				Completeness				Quality			
	E	S	M	L	E	S	M	L	E	S	M	L
<i>VGG Networks</i>												
VGG-11	31.0	28.6	22.9	41.7	45.4	42.5	34.7	64.0	17.6	16.3	13.0	23.7
VGG-16	41.3	31.5	38.2	34.7	63.5	45.9	57.4	50.2	23.5	17.9	21.7	19.7
VGG-16_bn	32.3	36.1	34.9	29.8	47.1	54.6	53.2	43.9	18.4	20.5	19.9	17.0
VGG-19	39.2	37.8	42.1	29.0	60.9	56.9	64.4	43.0	22.4	21.5	23.9	16.5
<i>Residual Networks</i>												
ResNet-18	27.7	33.0	35.7	26.5	41.3	48.1	54.2	39.7	15.8	18.8	20.3	15.1
ResNet-50	40.1	22.5	26.9	30.6	62.0	34.2	40.2	44.8	22.8	12.8	15.3	17.4
ResNeXt-50 32x4d	36.5	23.3	40.5	33.5	55.1	35.3	62.4	48.6	20.7	13.3	23.1	19.0
<i>Inception Networks</i>												
GoogLeNet	25.3	24.1	26.1	36.9	38.2	36.6	39.1	55.7	14.4	13.8	14.9	21.0
InceptionNet v3	25.7	24.9	38.6	40.9	38.7	37.5	57.8	62.9	14.7	14.2	21.9	23.3
<i>EfficientNet</i>												
EfficientNet_B0	33.9	31.9	34.8	35.9	49.2	46.5	48.9	49.8	19.3	18.1	19.5	21.3
EfficientNet_B7	23.7	39.0	41.3	43.4	35.9	58.3	60.9	61.8	13.5	22.2	24.0	25.6
<i>Uncategorized Networks</i>												
AlexNet	27.3	28.1	32.7	37.3	40.7	41.8	47.5	56.3	15.5	16.0	18.6	21.2
DenseNet-121	34.3	34.3	30.2	35.3	49.7	33.7	44.3	53.7	19.5	12.6	17.2	20.1
SqueezeNet	21.6	39.6	29.4	24.5	33.2	61.4	43.4	36.9	12.3	22.6	16.8	13.9

TABLE XI
Test accuracy on SVHN and STL-10 for downstream models using autoencoder encodings trained with different loss networks

Architecture	SVHN				STL-10			
	E	S	M	L	E	S	M	L
<i>VGG Networks</i>								
VGG-11	0.826	0.832	0.860	0.825	0.381	0.453	0.567	0.724
VGG-16	0.826	0.833	0.887	0.837	0.413	0.512	0.592	0.741
VGG-16_bn	0.816	0.820	0.863	0.492	0.434	0.318	0.247	0.465
VGG-19	0.826	0.833	0.896	0.821	0.397	0.499	0.607	0.736
<i>Residual Networks</i>								
ResNet-18	0.820	0.832	0.867	0.471	0.422	0.473	0.415	0.465
ResNet-50	0.821	0.833	0.862	0.571	0.413	0.554	0.413	0.480
ResNeXt-50 32x4d	0.819	0.830	0.864	0.259	0.419	0.383	0.428	0.403
<i>Inception Networks</i>								
GoogLeNet	0.814	0.868	0.849	0.595	0.373	0.474	0.540	0.593
InceptionNet v3	0.803	0.846	0.828	0.366	0.301	0.475	0.528	0.354
<i>EfficientNet</i>								
EfficientNet_B0	0.818	0.828	0.838	0.714	0.393	0.384	0.434	0.695
EfficientNet_B7	0.807	0.821	0.851	0.445	0.418	0.277	0.648	0.385
<i>Uncategorized Networks</i>								
AlexNet	0.818	0.817	0.799	0.744	0.387	0.596	0.640	0.669
DenseNet-121	0.758	0.831	0.862	0.264	0.442	0.488	0.565	0.578
SqueezeNet	0.825	0.845	0.843	0.791	0.405	0.513	0.639	0.681